The Role of the Primitive Relaxation in the Dynamics of Aqueous Mixtures, Nano-confined Water and Hydrated Proteins

S. Capaccioli[a*], K. L. Ngai[b], S. Ancherbak[a], P. A. Rolla[a], N. Shinyashiki[c]

[a]*Dipartimento di Fisica, Università di Pisa and CNR-IPCF, Largo Bruno Pontecorvo 3 ,I-56127, Pisa, Italy*
[b]*Naval Research Laboratory, Washington DC 20375-5320, USA*
[c]*Department of Physics, Tokai University, Hiratsuka, Kanagawa 259-1292, Japan*

Abstract

The relaxation scenario in aqueous systems, such as mixtures of water with hydrophilic solutes, nano-confined water and hydrated biomolecules, has been shown to exhibit general features, in spite of the huge differences in structure, chemical composition and complexity. Dynamics, in all these systems, invariably shows at least two relaxations: (i) a slower process, related to cooperative and structural motions of the water and solute molecules (in the case of mixtures) or related to interfacial processes in the case of confined water and (ii) a faster process, with non-cooperative character originating from water. The latter has properties including timescale and temperature dependence similar or related in all the aqueous systems. This water-specific relaxation can be identified as the primitive relaxation, or the Johari-Goldstein β-relaxation in glass-forming substances. The primitive process is the precursor of the many-body relaxation process which increases in length-scale with time until the terminal α-relaxation is reached.

Using new experimental data (at atmospheric and high pressure) along with a revision of most of the recent literature on the dynamics of confined water and aqueous mixtures, we show that the two above-mentioned relaxation processes are inter-related as evidenced by correlations in their properties. For instance, both relaxation time and dielectric strength of the water-specific relaxation exhibit a crossover from a stronger to a weaker dependence with decreasing *T*, at the temperature where the slow process attains a very long timescale (> 1ks) and becomes structurally arrested, exactly analogous to that found for β-relaxation in van der Waals liquids. Moreover, the primitive relaxation of water is shown to play a pivotal role in determining the dynamics of hydrated biomolecules in general, including the "dynamic transition" observed by neutron scattering and Mössbauer spectroscopy. We show that the primitive relaxation of the solvent is responsible for the dynamic transition, even in the case that the solvent is not pure water or an aqueous mixture.

PACS codes: 61.20.Lc, 61.43.Fs, 64.70.P-, 87.15.H-, 87.15.kr
Keywords: relaxation, water, aqueous mixtures, glass transition, hydrated proteins

1. Introduction

Water is the most common liquid on earth (it covers almost two thirds of the surface of the planet). It is also undoubtedly one of the most important substances without which life is

* capacci@df.unipi.it, Tel. +39-0502214322, Fax. +39-0502214333

Report Documentation Page

Form Approved
OMB No. 0704-0188

1. REPORT DATE	2. REPORT TYPE	3. DATES COVERED
2010		

4. TITLE AND SUBTITLE	5a. CONTRACT NUMBER
The Role of the Primitive Relaxation in the Dynamics of Aqueous Mixtures, Nano-confined Water and Hydrated Proteins	5b. GRANT NUMBER
	5c. PROGRAM ELEMENT NUMBER
6. AUTHOR(S)	5d. PROJECT NUMBER
	5e. TASK NUMBER
	5f. WORK UNIT NUMBER
7. PERFORMING ORGANIZATION NAME(S) AND ADDRESS(ES) **Dipartimento di Fisica,Universita di Pisa and CNR-IPCF,Largo Bruno Pontecorvo 3, I-56127,Pisa, Italy, ,**	8. PERFORMING ORGANIZATION REPORT NUMBER
9. SPONSORING/MONITORING AGENCY NAME(S) AND ADDRESS(ES)	10. SPONSOR/MONITOR'S ACRONYM(S)
	11. SPONSOR/MONITOR'S REPORT NUMBER(S)

12. DISTRIBUTION/AVAILABILITY STATEMENT
Approved for public release; distribution unlimited.

13. SUPPLEMENTARY NOTES
The original document contains color images.

14. ABSTRACT

The relaxation scenario in aqueous systems, such as mixtures of water with hydrophilic solutes, nano-confined water and hydrated biomolecules, has been shown to exhibit general features, in spite of the huge differences in structure, chemical composition and complexity. Dynamics, in all these systems, invariably shows at least two relaxations: (i) a slower process, related to cooperative and structural motions of the water and solute molecules (in the case of mixtures) or related to interfacial processes in the case of confined water and (ii) a faster process, with non-cooperative character originating from water. The latter has properties including timescale and temperature dependence similar or related in all the aqueous systems. This water-specific relaxation can be identified as the primitive relaxation, or the Johari-Goldstein β-relaxation in glass-forming substances. The primitive process is the precursor of the many-body relaxation process which increases in length-scale with time until the terminal α-relaxation is reached. Using new experimental data (at atmospheric and high pressure) along with a revision of most of the recent literature on the dynamics of confined water and aqueous mixtures, we show that the two above-mentioned relaxation processes are inter-related as evidenced by correlations in their properties. For instance, both relaxation time and dielectric strength of the water-specific relaxation exhibit a crossover from a stronger to a weaker dependence with decreasing T, at the temperature where the slow process attains a very long timescale (> 1ks) and becomes structurally arrested, exactly analogous to that found for β-relaxation in van der Waals liquids. Moreover, the primitive relaxation of water is shown to play a pivotal role in determining the dynamics of hydrated biomolecules in general, including the ?dynamic transition? observed by neutron scattering and M?ssbauer spectroscopy. We show that the primitive relaxation of the solvent is responsible for the dynamic transition, even in the case that the solvent is not pure water or an aqueous mixture.

15. SUBJECT TERMS					
16. SECURITY CLASSIFICATION OF:			17. LIMITATION OF ABSTRACT	18. NUMBER OF PAGES	19a. NAME OF RESPONSIBLE PERSON
a. REPORT **unclassified**	b. ABSTRACT **unclassified**	c. THIS PAGE **unclassified**		**29**	

Standard Form 298 (Rev. 8-98)
Prescribed by ANSI Std Z39-18

impossible. This explains the strong research interest on the structure and dynamics of water in the past and continued unabated till the present time. Notwithstanding, many fundamental aspects of its physico-chemical properties are still unexplained. Many anomalies of thermodynamic and dynamic properties of water become more pronounced in the metastable supercooled liquid state [r001]. In the literature, studies have been made on the dynamics of supercooled water in the region between melting point (273 K) and the homogeneous nucleation temperature (231 K) [r001, r002, r003, r004, r005]. There are also experimental evidences that water can exist also as an amorphous solid (glass) at very low temperatures (lower than 130 K), but once heated above the glass transition temperature, it transforms into a highly viscous liquids and then immediately crystallizes [r006, r007]. Therefore, dynamics of water is experimentally inaccessible for the liquid state in a wide temperature range (140 – 230 K at atmospheric pressure). In the literature, two alternative strategies are employed to obtain information in this region: (i) mixing water with hydrophilic glass-forming solutes, and (ii) confinement on the nanometer length-scale. Examples of some systems suitable to form homogeneous solutions with water (up to 50% in weight), that can be easily supercooled down to form a glass, are alcohols, ethylene and propylene glycols, sugars or carbohydrates (mono-, di- and polysaccharides) and some hydrophilic macromolecular systems, including biopolymers (from polypeptides to several proteins) [r008, r009, r010]. From the dynamic and structural properties of the water mixtures with variations of the solutes and concentrations, attempts were made to infer, by extrapolations, the properties of supercooled pure water in the unaccessible region below 230 K. Moreover, these studies is important *per se* because aqueous mixtures are often present in biological systems [r011] and the knowledge of the dynamics in their supercooled and glassy states is important in the field of cryoprotection of living organisms and biopharmaceuticals [r012]. The second strategy uses the nanoscale confinement in order to reduce the water molecular clusters down to sizes smaller than the critical size necessary for homogenous nucleation. Another effect of the confinement is the disorder induced by the interfaces that prevent the water molecules to form a crystalline lattice. Nanoconfined supercooled water was obtained in nanoporous systems as silica gels [r013], Vycor glasses [r014], zeolites, mesoporous molecular sieves [r015], and other systems. Crystallization does not occur in water dispersed in biorelevant materials, such as polymeric nanoporous hydrogels [r016], and in the water present in the hydration layer at the protein surfaces [r010, r017, r018].

The experimental findings reported in the literature on the dynamics of supercooled water are remarkably similar for most of the above mentioned systems, irrespective of the structure and chemical composition of the aqueous systems. At least two relaxation processes were always reported, both can be detected by the highly sensitive adiabatic calorimetry or by broadband dielectric spectroscopy [r008, r019]. There is a slower process coming from the structural relaxation of the solute molecules hydrogen bonded to water or from motion of molecules of the confining wall that are hydrogen bonded to water in the case of confined water. Its relaxation time has the Vogel-Fulcher-Tammann-Hesse (VFTH) *T*-dependence, typical of cooperative structural α-relaxation in glass-formers, and attains values between 10^2 -10^3 s at the glass transition temperature T_g, where a jump in heat capacity is observed by differential scanning calorimetry. Also present in the dielectric spectra at higher frequency is a faster process. From the increase of its dielectric strength with water content in the mixtures [r008, r020], as well as the increase of its relaxation time, on replacing the protonated water by deuterated water [r021], it is clear that the faster relaxation is a process originating specifically from the water component and has been called the ν-process [r008, r020]. The relaxation time τ_ν of the ν-relaxation shows qualitatively very similar features for many aqueous systems, almost universal, irrespective of the chemical and structural differences. Quantitative differences in τ_ν found for different solutes and concentrations are due to

variations in the hydrogen bonding of the water with the solute. τ_ν shows a marked crossover at some solute and concentration dependent temperature T_c from a Vogel-Fulcher-Tamman-Hesse temperature dependence to an Arrhenius one (with activation enthalpy around 50 kJ/mol for aqueous mixtures with higher water content) on cooling, resembling the Fragile-to-Strong transition already postulated for confined and bulk water [r022]. This crossover was alternatively ascribed as the consequence of the confinement of the water specific relaxation by the frozen glassy structure of the mixture at temperatures below T_c [r023]. Specifically, the authors of Ref.[r023] interpreted the ν-relaxation as the α-relaxation of the water component in the mixture, and assumed its length-scale increases monotonically with decrease in temperature. They argued that the increase cannot continue after temperature has fallen below T_c because of the finite size allowed by the frozen structure would stop the growth of the size of the cooperative rearranging region of the α-relaxation of the water component in the system [r023]. Yet according to other authors [r024, r025], the crossover is an apparent effect, due to merging of the primary and secondary relaxations of water at high temperatures together with a confinement-induced collapse of the strongly cooperative primary α-process of water near T_c~T_g. Therefore, below T_g only the secondary process of water would be effectively observed.

In the present paper, we propose a completely different interpretation, according to which the ν-relaxation in these systems is due to a specific process related to independent motions of water molecules in the presence of the solute or the confining wall. It is the analogue of the Johari-Goldstein (JG) secondary β-relaxation present in all glass-formers, which comes from motion of molecule individually and independently but as a whole [r026, r027]. Like JG β-relaxation of other glass-formers, the properties of the ν-relaxation are the same as the primitive relaxation of the Coupling Model (CM) [r008, r028]. The identification of the JG secondary relaxations of glass-formers with the primitive relaxation of the CM was confirmed from the good agreement between the observed τ_{JG} and the primitive relaxation time τ_0 [r028, r029]. According to the CM, the primitive relaxation is the precursor of the structural α-relaxation. The latter is the product of the development of the many-body dynamics with time, starting from the primitive realxation. Thus there is a strong correlation between the two processes, and CM predicts the following relation between τ_α and τ_{JG} or τ_0 [r028]:

$$\tau_{JG} \approx \tau_0 = \tau_\alpha^{(1-n)} t_c^n \qquad (1)$$

where $t_c \approx 2$ ps in molecular glass-formers, and n is the coupling parameter related to the exponent β_K of the Kohlrausch correlation function for the α-relaxation by $(1\text{-}n) \equiv \beta_K$ [r030]. Therefore the power law relation between the two timescale given by Eq.(1) is expected. As in the case of binary van der Waals liquids [r027], the observed faster ν-process in aqueous mixtures is the primitive relaxation or the JG β-relaxation of the water component both above and below T_g. It is well known that τ_α has a VFTH temperature dependence above T_g, which changes to Arrhenius dependence T_g, after entering into the structurally arrested glassy state [r027]. From this, it follows immediately from Eq.(1) that we have a similar change in T-dependence of τ_ν when crossing T_g.

The purpose of the present paper is given as follows. First, new experimental data from dielectric spectroscopy on aqueous mixtures together with a critical re-examination of published results are used to show that the interpretation of ν-relaxation as the primitive relaxation of water is in full agreement with the temperature, pressure, concentration dependence of its dynamic features. On the contrary, we will show how the other mentioned interpretations [r022, r023, r024, r025] are not fully compatible with the experimental results. Then, some examples of dynamics in nano-confined water systems are presented to show similar properties as aqueous mixtures, and the same explanation applies. Finally, the concepts verified on the aqueous mixtures will be used for elucidating the role of the

primitive relaxation of water or solvent in general on the dynamics of hydrated proteins including the dynamic transition observed by neutron scattering and Mössbauer spectroscopy.

2. Experimental

New data on the dynamics of water in glass-forming mixtures were obtained by dielectric spectroscopy in the frequency range from 10 mHz to 10 GHz, by means of a combination of the Novocontrol Dielectric Analyser and the Agilent Network Analysers 8722D and 8753ES. Dielectric study was carried out in the temperature range from liquid to the glassy state on cooling by isothermal steps, from 310 K down to 110 K, after an appropriate equilibration time. The new systems investigated and here presented are the monosaccharide 2-Deoxy-D-ribose, mixed with 32% wt. fraction of water, and the heptamer of polypropylene glycol, with M_w=400 Da (PPG400), mixed at different water fraction (from 4% to 45% wt.). Both hydrophilic solutes were obtained from Sigma-Aldrich and used as received. Distilled and deionized water (electric conductivity lower than 18.3 μS m^{-1}) was prepared by an ultra-pure water distiller (Millipore, MILLI-Q Lab). Both mixing of components and loading of the sample holder were performed in controlled atmosphere (dry nitrogen). In addition to these data, in this paper we present new analysis of results on other systems obtained by our groups, part of which have already been published. These are the oligomers of ethylene glycols (EG) [r031, r032, r033], one mixture of PPG400 under high pressure [r034], glycerol-water mixtures [r008], and hydrated Bovine Serum Albumin [r035]. Experimental details in these other systems can be found in the papers cited.

3. Water dynamics in mixtures and nano-confinement

3.1 Dynamics of Aqueous Mixtures

Fig.1.a shows the relaxation map of a mixture of 35% wt. fraction of water in the ethylene glycol oligomer with 5 repeat units (5EG). The typical scenario with two relaxation processes is evident. The slow process has the Vogel-Fulcher-Tammann-Hesse (VFTH) *T*-dependence, typical of cooperative α-relaxation and responsible for glass transition of the mixture. The cooperative character can be confirmed by the value of the dielectric relaxation time at the calorimetric glass transition T_g [r033] (172 K), that is $\tau_\alpha(T_g)\sim10^2$ s. Concerning the ν-relaxation, it has an Arrhenius *T*-dependence at low temperature with an activation enthalpy of 49 kJ/mol, similar to the value of about 50 kJ/mol universally found in the glassy aqueous mixtures [r008]. On increasing temperature, at T_c =169 K, τ_ν changes to assume a stronger *T*-dependence. This crossover does not occur at 220 K as predicted in ref.[r022]. On the contrary, it occurs always few degrees below T_g, where τ_α exceeds 1-10 ks, where it can be identified in every aqueous mixtures investigated before. For instance, the same scenario can be found in deoxyribose mixed with 32% wt water fraction (see Fig.2(a)): in this case the crossover of τ_ν occurs at T_c =182 K, while T_g =185 K. Again, in the glassy state τ_ν has an Arrhenius *T*-dependence with the activation enthalpy of 51.5 kJ/mol. Dielectric strengths of both processes are plotted in Fig.1.b and Fig.2.b. Dielectric strength can be expressed as:

$$\Delta\varepsilon = \frac{4\pi}{3k_BT}\frac{N}{V}Fg_K N_A\left\langle\mu^2\right\rangle \qquad (2)$$

where N_A is the Avogadro number, *F* is a numerical factor related to the local field correction,

T is the temperature, g_K is the Kirkwood factor, V the specific volume, $(<\mu^2>)^{1/2}$ the effective dipole moment (i.e. the component $\mu \cdot \sin(\theta)$, where θ is the mean reorientation angle), N is the number of active dipoles [r036]. For structural relaxation, N/V is almost constant and $\Delta\varepsilon_\alpha$ increases linearly with $1/T$. On the other hand, $\Delta\varepsilon_\nu$ of the ν-process increases with T and this is evidence for increase with temperature of either the number of active dipoles or the reorientation angle of the ν-process. Moreover, $\Delta\varepsilon_\nu$ exhibits a change to a stronger increase with increasing T after crossing T_g.

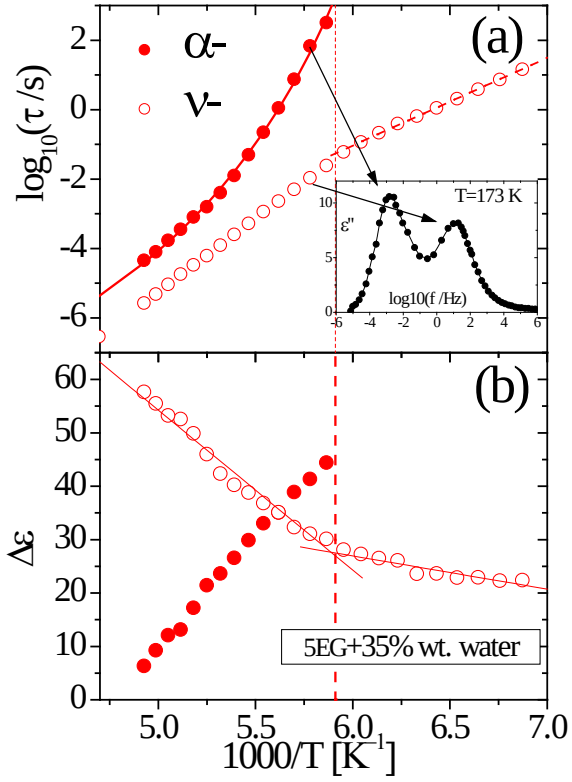

Figure 1. a) Plot of relaxation times vs. reciprocal T of 35% wt. fraction of water in 5EG. Close and open red symbols indicate the α- and ν- process, respectively. Solid line is the VFTH function fit, dashed line is the Arrhenius fit to the data in the glassy state. The vertical line indicates the temperature where τ_α=1 ks. Inset shows the loss spectra for T=173 K. b) Plot of dielectric strength vs. reciprocal T for the α- and ν- processes. Symbols are the same as in panel (a). Lines are from linear regression for data above and below T_g.

These features of the ν-process are typical of the secondary β-relaxation in glass-forming systems [r008]. A combined study of NMR and dielectric spectroscopy in polyols [r036] demonstrated that there is an empirical relationship between the ratio of dielectric strength of secondary β- over structural α-relaxation and the cone semiangle θ related to dipole jump reorientation:

$$\frac{\Delta\varepsilon_\beta}{\Delta\varepsilon_\alpha} = (\sin\theta)^2 \qquad (3)$$

In the glassy state, the spatial restriction of local motion is reflected by the low and almost constant (or weakly increasing) value of $\Delta\varepsilon_\beta$, whereas larger reorientation amplitude is possible above T_g, and hence the stronger T-dependence of $\Delta\varepsilon_\beta$ is observed. Identifying the ν-relaxation as a secondary process is fully compatible with its dielectric strength behavior. Nevertheless, we have to bear in mind that it is a water-specific process with hydrogen bonding to the solute. Therefore, some differences in details of the motion of water in the ν-

relaxation compared with secondary relaxation in van der Waals liquids and polymers can be expected. For instance, in organic glass-formers, the ratio of dielectric strengths of Eq.(3) close to T_g is often quite small (0.08 is the maximum value reported in [r036]), while in water specific process the ratio between $\Delta\varepsilon_\nu$ and $\Delta\varepsilon_\alpha$ can be of the order of unity (see for instance Fig.1.b and Fig.2.b), corresponding to large jump reorientation angle in the glassy state and possible participation of translation above T_g. Such large angle comparable to the tetrahedral angle expected from the dielectric strength of the ν-relaxation have actually been found by NMR in hydrated biomolecules [r048]. Actually this result is not surprising if we consider that water is the smallest molecule in Nature that involves hydrogen bonding. The mechanism of this water specific JG relaxation is therefore quite different from the JG relaxation in van der Waals glass formers and polymers. After breaking two hydrogen bonds, as suggested by the activation energy≈52 kJ/mol of the ν-relaxation in most aqueous systems, the water molecule is free to rotate and translate and there is no reason that local reorientation of the small water molecule has to be restricted to small angles, especially above the T_g of the host system.

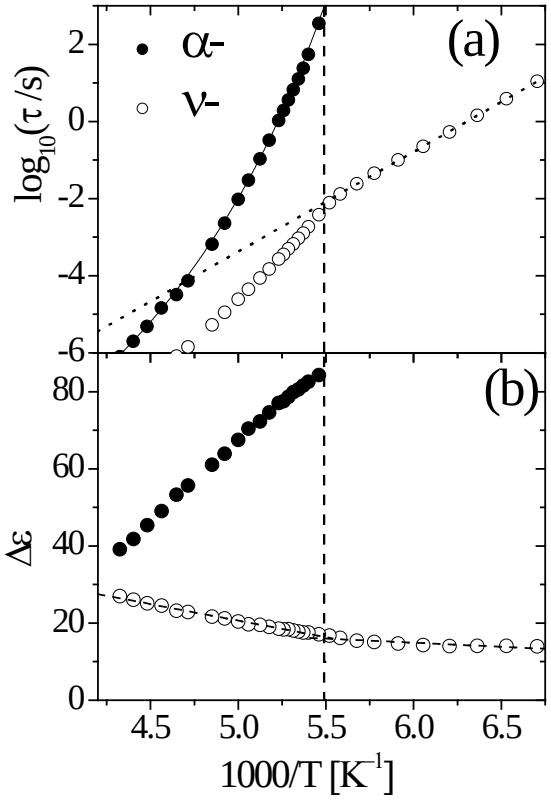

Figure 2. (a) Plot of relaxation times vs. reciprocal temperature of 32% wt. fraction of water in deoxyribose. Close and open black symbols indicate α- and ν- process, respectively. Solid line is the VFTH function fit, dotted line is the Arrhenius fit to the data in the glassy state. The vertical line indicates the temperature where τ_α=1ks. b) Plot of dielectric strength vs. reciprocal temperature for the α- and ν- processes. Symbols are the same as in panel (a). Lines are from linear regression for data above and below T_g.

The analysis of dielectric strength, often overlooked in literature for its importance, helped in identifying the water-specific ν-relaxation truly as the secondary relaxation. In particular, the increase of $\Delta\varepsilon_\nu$ with T is a clear evidence that its secondary relaxation character continues to temperatures above T_g, where τ_ν has already changed its temperature dependence to VFTH-like from the Arrhenius dependence below T_g. It is worthwhile to point out that both the

changes from a weaker to a stronger *T*-dependence on crossing T_g observed for τ_ν and $\Delta\varepsilon_\nu$ in aqueous mixtures are exactly analogous to that found for the secondary relaxation of a fast component in binary van der Waals liquids [r027, r037, r038, r039], suggesting similar interpretation. The behaviour of $\Delta\varepsilon_\nu$ invalidates the suggestion by others [r021, r023, r040] that the observed water-specific relaxation is the α-relaxation of the water component in the mixture, with its relaxation time having the usual VFTH *T*-dependence above T_g, but it becomes confined below T_g to assume the Arrhenius *T*-dependence. It is remarkable that the dynamics of water process in deoxyribose+water mixture published in Ref.[r040] with behaviour similar to Fig.2 was interpreted according to this idea, even though this interpretation cannot be reconciled by the temperature dependence of $\Delta\varepsilon_\nu$ found in the data of Ref.[r040] as well as in our data as shown in Fig.2(b).

Actually, even for van der Waals and polymeric liquids confined in nanoporous systems [r041], a milder crossover for τ_α than that experienced by τ_ν is usually found as a consequence of the finite size effect from confinement. However unlike aqueous mixtures, in these confined systems, $\Delta\varepsilon_\alpha$ was never found increasing with *T* in the temperature range where the effect of confinement on the α-relaxation has not set in (i.e., τ_α has the VFTH dependence) [r041]. Thus, the temperature dependence of $\Delta\varepsilon_\nu$ is different from that of $\Delta\varepsilon_\alpha$ van der Waals liquids and polymers under nano-confinement. This demonstrates the explanation of the ν-process in aqueous mixtures as the α-relaxation of water unconfined above T_g and confined below T_g [r021, r023, r040] contradicts the data of the nano-confined van der Waals liquids and polymer.

Finally, the increase of $\Delta\varepsilon_\nu$ with *T* in the whole temperature range is not compatible with the interpretation by other authors [r024, r025] either, according to which the water-specific relaxation is a merged α- and β-process above T_g and only the β-character survives in the glassy state. If so, dielectric strength of water-related ν-process should decrease with T above T_g. Actually this interpretation is refuted by the data in some aqueous solutions, where both the α- and ν-process are present and well separated from each other above T_g (see inset in Fig.1): the fact that the ν-process is well separated from the α-process way above T_g rules out merging of the two processes and splitting apart occurring just in vicinity of T_g. The same authors [r021] claimed also that the change of slope of τ_ν on crossing T_g could be nothing but an apparent effect due to the fitting procedure. This could happen in the case where α- and β-timescales are close each other and the results could depend on the deconvolution method used. In reality, there are several examples of typical secondary relaxations of organic compounds where no merging with the α-process occurs at temperatures high above T_g, and the change of temperature dependence of its relaxation time τ_β is real because the two relaxations are widely separated at T_g and no fitting procedure is needed to determine τ_β. Examples include the studies by Kessairi et al. [r027] and by Blochowicz et al. [r038] on component dynamics of binary mixtures where a clear change of activation energy of τ_β at T_g was reported. Another example is sorbitol and xylitol subjected to high pressure studies by Paluch and co-workers [r042]. In all the mentioned cases and other examples, the secondary relaxation time changes its Arrhenius *T*-dependence in the glassy state after crossing T_g. This effect was seen directly without the use of any fitting procedures, such as the so-called "Williams-ansatz" or by simple superposition of the two processes. Even in this case of well resolved α- and β-relaxations, by subjecting the data to analysis by the Williams-ansatz procedure, Blochowicz found the change of activation energy of τ_β at T_g [r038]. According to such procedure, the total correlation function can be expressed in the time domain as a linear combination of the α-correlation function and a product between α- and β-correlation function:

$$\Phi(t) = a\Phi_\alpha(t) + (1-a)\Phi_\alpha(t)\Phi_\beta(t) \qquad (4)$$

As a consequence, in the frequency domain eq.(4) gives rise to the usual superposition of two loss peaks, but with the faster one being an "effective" secondary relaxation peak, resulting from the convolution in Fourier transform. In principle, α- with β- relaxation time could have any kind of temperature dependence (see for instance ref.[r038]), but many authors [r043, r044] arbitrarily fix τ_β to have an Arrhenius behaviour for all temperatures. If the β-relaxation would have an Arrhenius behaviour in the whole temperature range, when its timescale approaches that of the α- (with a VFTH behaviour), a change of the temperature dependence of the "effective" secondary relaxation to a stronger dependence than the assumed Arrhenius dependence of τ_β could be expected. It is worthwhile to point out that the Williams-ansatz is an hypothesis that has not yet been given a proof to be fundamentally correct, and also its assumption that $\Phi_\alpha(t)$ and $\Phi_\beta(t)$ are independent functions seems to contradict the experimentally observed connection between the α- and β- relaxation as demonstrated in refs. [r045, r029, r046]. Moreover, we stress that in several examples where the secondary relaxation time deviates from the temperature behaviour of the glassy state, the separation between structural and secondary relaxation in their relaxation times is quite large, more than five decades at ambient pressure and even larger at very high pressure. We can see such examples from the mixture, PPG400+26% wt. fraction of water, in Fig. 3, where the supposed influence of the α-relaxation should be negligible on the much faster timescale of the secondary ν-relaxation. Whether at ambient or elevated pressure, the change in *T*-dependence of τ_ν occurs at T_g, which increases with pressure. Concomitantly, the separation between α- and ν-processes increases with pressure [r034] and the $\tau_\nu(T_g)$ at the crossover becomes shorter on increasing pressure, at odds with the prediction of recent theories [r047].

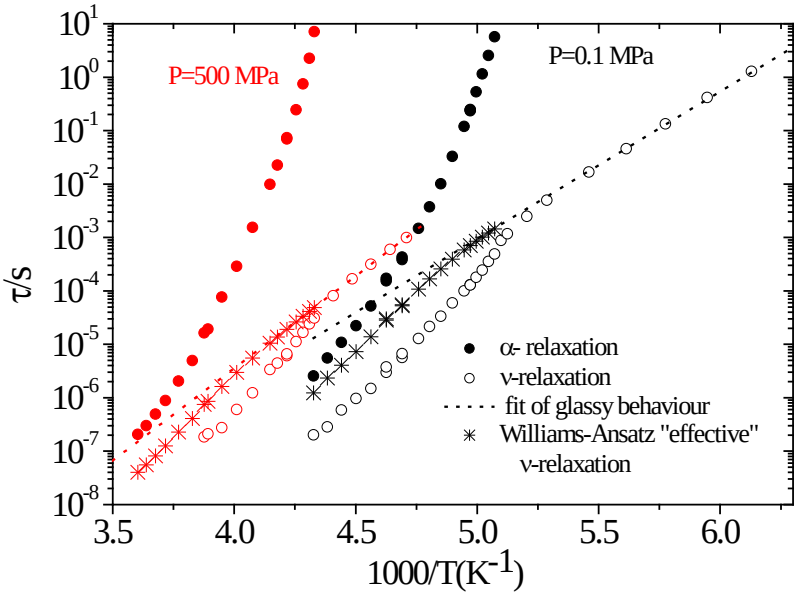

Figure 3. Semilog Plot of relaxation times vs. reciprocal T of 26% wt. fraction of water in PPG400. Close and open circles indicate α- and ν- process, respectively. Asterisks are the relaxation times of the "effective" relaxation obtained from the convolution procedure indicated by the Williams Ansatz. Black and red symbols indicate isobaric scan done at P=0.1 and 500 MPa, respectively. Dotted lines are Arrhenius fits to the data in the glassy state.

The data in Fig.3 offers an opportunity to test the effect of the convolution of the α- and β-

relaxations according to the Williams ansatz. We used the same procedure described in Refs.[r043, r044]. First we determined the Arrhenius T-dependence of the ν-relaxation time in the glassy state, then we extrapolated this dependence to higher temperatures up to where it merges with the α-relaxation. Following Eq.(4), we calculated the "effective" relaxation time for the convoluted of α-and ν-relaxation, and examined whether it can account for the observed change in *T*-dependence of τ_ν. The "effective" ν-relaxation times from this exercise using the Williams ansatz are shown in Fig.3. It is clear by inspection of Fig.3 that the Williams ansatz analysis brings only a milder deviation of the "effective" ν-relaxation times from the Arrhenius behaviour and at temperature significantly higher than T_g. These results are both in disagreement with experimental observation, and therefore the Williams ansatz is not able to explain the large deviation from the Arrhenius dependence of τ_ν after crossing T_g which is experimentally observed at ambient and elevated pressures.
On the other hand, if we interpret the ν-process as the primitive JG relaxation of water, its connection to the structural relaxation expressed by eq.(1) naturally explains why the *T*-dependence of τ_ν has a crossover at T_g. It simply reflects a similar but well known change of behaviour experienced by the structural relaxation on entering in the glassy state.

Although the features of the dynamics of aqueous mixtures discussed so far are analogous to binary van der Waals liquids and explained in similar way by the CM, there is however a slight difference between these two systems. It is noteworthy that each component of binary van der Waals liquids could have its own distinct α- and JG β-relaxations [r053, r120], hydrogen bonding of water with the hydrophilic solute in aqueous mixtures forces the motions of the two components to be coupled together, on both the slow and the fast time scales.

The effect of such coupling at the short timescale and at the local scale can be evidenced by several results in aqueous mixtures and, more specifically, in protein systems (see Section 4). In fact, the motion of water involved in primitive relaxation is coupled to some local motion of the solute because of hydrogen bonding between water and the solute, especially at low water concentration. Evidence of this coupling can be seen from the sensitive dependence of τ_ν and its activation energy on the concentration of water in the mixtures, or from the different values shown by τ_ν in mixtures with different solutes [r008]. First, we show by examples the effect of water concentration on τ_ν. It is a very general trend reported before in literature (see for instance [r021]). At any fixed temperature, the relaxation time τ_ν decreases on increasing the concentration of water in the mixture. The decrease of τ_ν continues until at very high molar concentrations of water where it approaches down to some limiting value which is more or less independent of the specific solute. This dependence of τ_ν on composition of aqueous mixture can be readily explained by the fact that, at very low water molar concentration, water molecules are mainly hydrogen bonded to hydrophilic groups of the solute, which usually has lower mobility than water molecule, whereas at high water molar concentration the environment of water molecule is mainly composed of the more mobile water molecules themselves. In the latter case, the activation energy in the glassy state for the relaxation time τ_ν is about 52 kJ/mol, which is not much larger than the energy of breaking two hydrogen bonds to enable local relaxation of water. Not so well publicized is that the position of τ_ν in aqueous mixtures at low water concentration is very close to that of the primitive relaxation of the pure system. We can show two examples in Fig.4 and Fig.5.

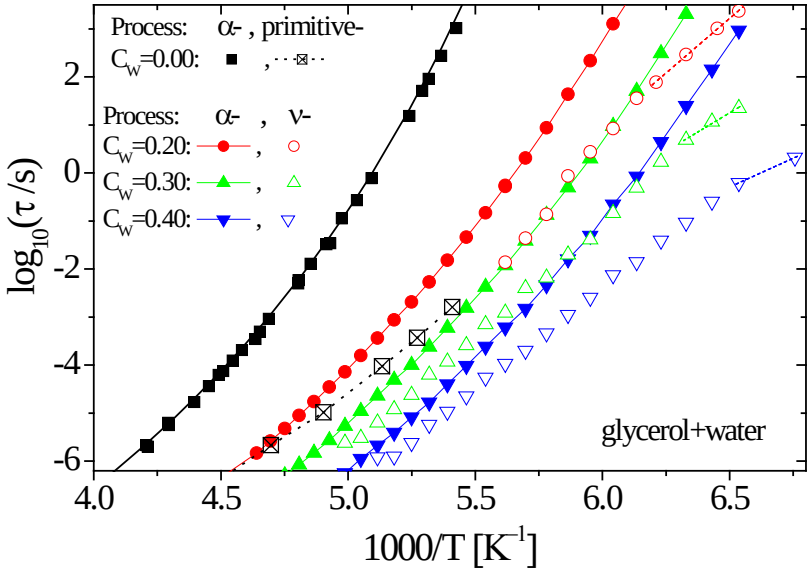

Figure 4. Plots of relaxation times vs. reciprocal T of glycerol-water mixtures at different water weight fraction C_W. Close and open symbols indicate α- and ν- process, respectively. The crossed black squares represent the primitive relaxation time for anhydrous glycerol as obtained by application of CM according to eq.(1). Solid lines are VFTH function fits, dotted lines are Arrhenius fits to the data in the glassy state.

Fig.4 shows the relaxation times for glycerol-water mixtures at different water weight fraction C_W. Both α- and ν- relaxation processes are present in the mixtures at different C_W, with the same characteristic behaviour already illustrated in Fig.1 and Fig.2. On increasing C_W both processes are moving to lower temperature, as a consequence of the plasticization effect due to water. The crossover of τ_ν occurs always few degrees below T_g, and the activation energy in the glassy state approaches that one characteristic of ν-relaxation. Data for anhydrous glycerol are taken from ref. [r049]. From those data, the relaxation time predicted for primitive process by eq.(1) can be estimated for the anhydrous glycerol. The ν- relaxation time τ_ν in mixtures at low C_W is very close to the primitive relaxation time of anhydrous glycerol. At higher C_W, τ_ν move to shorter times when the interactions of water with the solute becomes less important. Another example is shown by Fig.5, where relaxation times of mixtures of water with PPG400 are plotted, as well as the data for anhydrous PPG400 [r050]. For anhydrous PPG400, a true JG β-relaxation was identified (with relaxation time τ_{JG} in agreement with the CM predictions for the primitive relaxation time τ_0 from Eq.(1)), as well as an additional secondary γ-process having much shorter relaxation times and originating from intra-molecular degrees of freedom. At low C_W, the interaction of water molecule with its environment comprised mainly of PPG400 affects the motions of the ν-relaxation. The water molecule can be considered to serve as a "probe" of the local dynamics of the solute, and hence the primitive motions of the solute are reflected in the ν-relaxation. For example at the low water fraction of C_W=0.04, it is evident from Fig.5 that τ_ν is not much smaller than τ_{JG} or τ_0 of the pure solute. This can be considered as evidence of the ν-relaxation is to some degree coupled to the environment and its local dynamics. On increasing the concentration, the ν-relaxation becomes faster to approach the ν-relaxation time of pure water confined in two layers on the surface of vermiculite clay [r051, r052], molecular sieves [r055], silica gels [r059], and graphite oxide [r068] (see next sub-section). The ν-relaxation with Arrhenius T-dependence and activation energy ~ 50 kJ/mol observed in aqueous mixtures at high molar

concentration of water can be considered as approximately the same as the primitive or JG β-relaxation in bulk water, which cannot be observed over the same temperature range because of crystallization.

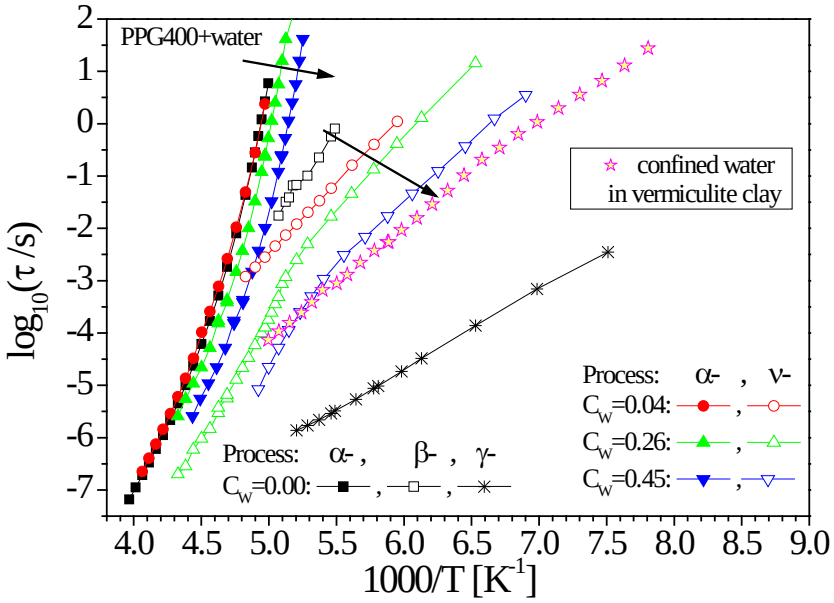

Figure 5. Plots of relaxation times vs. reciprocal T of PPG400-water mixtures at different water weight fraction C_W. Close and open symbols indicate α- and ν- process, respectively. The black asterisks represent the γ relaxation times of anhydrous PPG400. Stars are data for water confined in vermiculite clay [r051, r052]. Arrows show the evolution with increasing C_W.

Another example of coupling of the ν-relaxation to its environment comes from aqueous mixtures with the same water mass fraction C_w=0.35 but with the solute that are oligomers of different molecular weights or degree of chain connectivity, such as the ethylene glycols oligomers nEG (with n=2, 3, 4, 5, 6) and PEG400 [r031, r032, r033]. Shown in the upper panel of Fig.6 are the relaxation times of the α-process involving cooperative motions of solute and water altogether and the fits to their *T*-dependences by the VFTH relation. The lower panel shows the water-specific ν-relaxation. Each vertical line marks the glass transition temperature T_g at which τ_α=1 ks. Below T_g, the structure is arrested, and τ_ν changes to assume the Arrhenius *T*-dependence with activation energy close to 50 kJ/mol, similarly for all the systems. The temperature at which the change occurs, $T_c \approx T_g$ increases with the molecular weight of the oligomers, and concurrently $\tau_\nu(T_g)$ decreases.

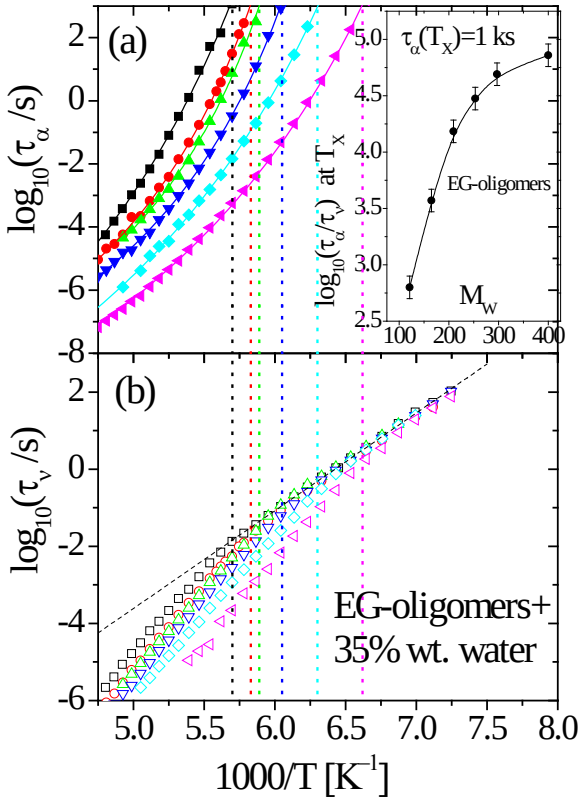

Figure 6. (a) Plots of α-relaxation times vs. *1000/T* of 35% wt. fraction of water in nEG: black squares (PEG400), red circles (6EG), green up triangles (5EG), blue down triangles (4EG), cyan diamonds (3EG) and magenta left oriented triangles (2EG). Solid lines are VFTH function fits, vertical dotted lines indicate the temperature where τ_α=1ks. (b) Plots of ν-relaxation times vs. *1000/T* for the same systems as in panel (a). Open symbols are related to the same quantities represented by solid symbols in panel (a). The black dotted line is Arrhenius fit to the data of PEG400/H_2O in the glassy state. Inset shows the timescale separation between α- and ν- processes vs. molecular mass of the EG oligomer, curve is a guide for the eye.

CM can rationalise these properties. It has been generally demonstrated in binary mixtures of van der Waals liquids that the coupling parameter *n* of the α-relaxation of the more mobile molecule increases on decreasing the mobility of the other component. That is also the case of the nEG systems of Fig.6, where the molecular weight increases and the concentration of water is kept constant. The steepness or fragility index *m*, defined by $d\log_{10}(\tau_\alpha)/d(T_g/T)$ evaluated at (T_g/T)=1 usually correlates with *n*, the degree of cooperativity of the α-process [r054]. In the nEG-water mixtures, *m* was found to increase with molecular weight of the solute nEG from 58 (2EG) to 67 (6EG) [r033], and hence also *n*. According to Eq.(1), a larger coupling parameter *n* makes the τ_ν shorter at any fixed value of τ_α such as $\tau_\nu(T_g)$=1 ks. That is exactly what happen for ν-relaxation in nEG+water mixtures, i.e., the separation in timescale of the two relaxations given by $\log_{10}(\tau_\alpha/\tau_\nu)$ at fixed τ_α=1 ks, increases as the molecular weight of the solute increases (see inset of Fig.6). It is important to stress that, in spite of the differences in molecular weight of the solute, τ_ν does not show large variations, especially below T_g. On the other hand, the primary α-relaxation time of these mixtures are immensely different because of their VFTH-like temperature dependences and widely different glass transition temperatures T_g, as well as different steepness indices *m*. The inset of Fig.6 suggests that if we extrapolate the trend of the decrease of $\log_{10}(\tau_\alpha/\tau_\nu)$ with the decrease in the molecular weight of the ethylene glycol oligomers down to M_w=62.1 for 1EG, its value of

$\log_{10}(\tau_\alpha/\tau_\nu)$ and hence n will be smaller. Replotting the data of $\log_{10}(\tau_\alpha/\tau_\nu)$ against the number of carbons can let us extrapolate it down to zero carbon of a hypothetical solute resembling water, which has even lower values of $\log_{10}(\tau_\alpha/\tau_\nu)$ and n than aqueous mixtures of 2EG and 1EG. If this hypothetical solute can be likened to water, the results suggest the structural α-relaxation of water has a very low degree of cooperativity or small n, and τ_α is not much longer than τ_ν than found in aqueous mixtures of 2EG and 1EG. The exercise suggests that water is not a "fragile" liquid as inferred by others from other experimental facts [r080, r121, r122].

The discussions given above have made clear the interrelation between α- and ν-relaxation process and the properties of the water-specific nature of the primitive ν-relaxation. The dynamics of water are very similar in different systems, irrespective to the chemical and structural composition of the mixtures. The interpretation and explanation are generally applicable to various situations. The results and the understanding of them gained will be very useful in tackling the dynamics of hydrated proteins and biomoleucles in Section 4, which are more complex because of these systems are spatially inhomogeneous. Before that, as another application of the CM prediction based on the primitive relaxation of water, we now analyse the ν- relaxation in confined water systems.

3.2 Dynamics of nano-confined water

A strategy that has been often used to study the dynamic properties of water in the metastable supercooled state at very low temperatures is to confine it at the nanoscale, in order to reduce the water molecular clusters down to smaller sizes than the critical one to have an homogeneous nucleation. Another effect of the confinement is the order/disorder induced by the interfaces that can prevent the water molecules to form a crystalline lattice. Of course, the chemical and physical interactions of the interfacial water layer with the hard confinement imposed by the nano-structured matrices can strongly modify the dynamics with respect to the bulk case: water dynamics can be affected even above the supercooled regime and additional processes can be originated. Despite these differences with the bulk case, the study of the dynamics of nano-confined water is of great interest. Among the several examples of supercooled water obtained in confined systems we could mention water confined in nanopores of Vycor glasses [r014], in nanoporous silica gels [r013], in silica hydrogels [r059, r060, r061], in nanoporous silica matrices MCM-41 [r015, r022, r056, r058], in molecular sieves [r055, r057], in vermiculite clays [r051, r052], in poly(HEMA) hydrogels [r016, r062, r063, r064, r065], water trapped in zeolites [r066, r067] or intercalated in graphite oxide [r068]. The study of dynamics often involves a wide timescale range, using a combination of different techniques, such as dielectric spectroscopy, neutron scattering, modulated or adiabatic calorimetry. Restricting our analysis to dynamic data obtained by dielectric spectroscopy, an analysis similar to that of the previous subsection on water mixtures can be performed. We recall here a couple of paradigmatic examples of confined systems.

The dynamics of water nano-confined in cylindrical pores with diameter of 10 Å of molecular sieves (MS) was studied by means of dielectric spectroscopy [r055]. Two major relaxation processes were observed in dielectric spectra (see Fig.2b in Ref.[r055]): one slower (s) and one faster (f). The slower (s) process is much more intense and it is contributed by most of the water molecules in 10 Å pores: it was attributed by authors of ref.[r055] to strong interactions of water with the hydrophilic inner surfaces of molecular sieves. Its relaxation time, τ_{sMS}, strongly increases with decreasing temperature up to reach 100 s around 170 K (see Fig.7). The relaxation time of the weaker and faster (f) process, τ_{fMS}, has Arrhenius temperature dependence at temperatures lower than 175 K (similarly to what shown for water

confined in vermiculite clay [r051, r052], see Fig.5) but changes to stronger temperature dependence at higher temperatures. Such crossover of the temperature dependence of τ_{fMS} in the vicinity of the temperature where τ_{sMS} exceeds the experimental equilibrium time is similar to what we have shown for the τ_v of the water JG-process in various aqueous mixtures (see §.3.1 and [r008]), and it is a general property of JG β-relaxation in glass-forming systems. Such similarity could suggest to interpret the faster process observed for MS confined water as the primitive relaxation or the JG β-relaxation of water and the associated slower process as the α-process of water strongly interacting with the hydrophilic inner MS surfaces. If this interpretation is valid, then τ_{fMS} and τ_{sMS} for water confined in 1.0 nm MS pores should obey to the strict relation between τ_{JG} and τ_α, respectively, predicted by the coupling model (CM) (see Eq.1) [r028, r029, r039, r053]. Applying the CM relation adapted for the present case we can obtain the prediction for τ_{sMS} from the data of τ_{fMS}: $\tau_{sMS}(T)=[t_c^{-n}\tau_{fMS}(T)]^{1/(1-n)}$. If we choose n=0.31, the calculated τ_{sMS} well agree with the experimental values (see Fig.7). Such value of $\beta_K\equiv(1-n)=0.69$ is not far from the value of 0.65 reported by Swenson et al. [r057] as the Kohlrausch exponent obtained on the same MS system by means of quasi-elastic neutron scattering after averaging the results from various scattering vectors *Q*.

Another good example of the presence of slow and fast processes related to water dynamics in confined systems is the case of water confined in nano-porous matrices MCM-41. Recent dielectric data [r056] report the existence of a fast relaxation process for water confined in nanoporous silica matrices MCM-41-C10 with pore diameter 2.14 nm at hydration levels with h=0.12, 0.22, 0.55. Results are shown in Fig.7, where a comparison to the MS data reveals that the water relaxation times in MCM-41 are close to τ_{fMS}. Moreover, also in the MCM-41 case there is a change of T-dependence of relaxation time, located at nearly 166 K (1000/T(K)=6), paralleling what happens in molecular sieves. The similarity to what shown previously for other systems should suggest that the relaxation (red open symbols in Fig.7) obtained by dielectric spectroscopy for water confined in MCM-41 is the JG β-relaxation of water. If so, we should aspect to find also an associated slower α-process, attaining a very long time at ≈166 K. Unfortunately, the low frequency side of dielectric spectra is usually masked by the d.c. conductivity contribution, but a slow process loss peak can be revealed from the dielectric spectrum at 220 K after subtracting off the conductivity [r056]. The relaxation time so deduced is very similar to what found for τ_{sMS} (see Fig.7). Our idea is that the fast process observed in water confined in both MS and MCM-41 nano-pores is the primitive or JG β-relaxation time of water and that a related slow or α-relaxation exists whose relaxation time is 10^3 s around 166 K, where the fast process time exhibits the crossover in the T-dependence. A further support to this interpretation comes from recent adiabatic calorimetry measurements of the enthalpy relaxation of water confined within 1.2 nm MCM-41 nano-pores made by Oguni and coworkers [r015]. From the enthalpy traces a faster and a slower relaxation have been found. Their relaxation times, τ_{fMCM} and τ_{sMCM}, have the value of 10^3 s at T=115 and 165 K, respectively, and are shown in Fig.7 by the two large circles. τ_{sMCM} is about the same at 10^3 s as that of τ_{sMS} from dielectric relaxation of water confined in molecular sieves with pore diameter of 10 Å [r055], that should be also similar to the slow process in MCM-41 (see solid triangle in Fig.7). On the other hand, the temperature location of $\tau_{fMCM}=10^3$ s from adiabatic calorimetry is 115 K, that is nearly the same as that obtained by extrapolating the Arrhenius dependence of the time of the fast relaxation process determined by dielectric relaxation [r056] to 10^3 s, as demonstrated in Fig.7. Such agreement shows that relaxation times from both methods belong to the same process. The fast process of water in molecular sieves and MCM nanopores has very general features similar to those of other aqueous systems: it has about the same activation enthalpy as τ_{JG} (or τ_v) of the 50% water

mixtures with PVME, PVP, and other water-polymer mixtures shown in Ref.[r008], as well as for the 6 Å water layer confined in fully hydrated Na-vermiculite clay [r051]. Moreover, the τ_{fMCM} from adiabatic calorimetry located at T=115 K is nearly the same as the value obtained by extrapolation of the Arrhenius dependence of τ_{JG} of the 50% water mixtures with PVME or with PVP to lower temperatures [r008]. All these coincidences indicate that the fast relaxation observed by dielectric relaxation and adiabatic calorimetry is an intrinsic feature of water, i.e. its primitive relaxation or JG β-relaxation, present in mixtures and in nano-confinement.

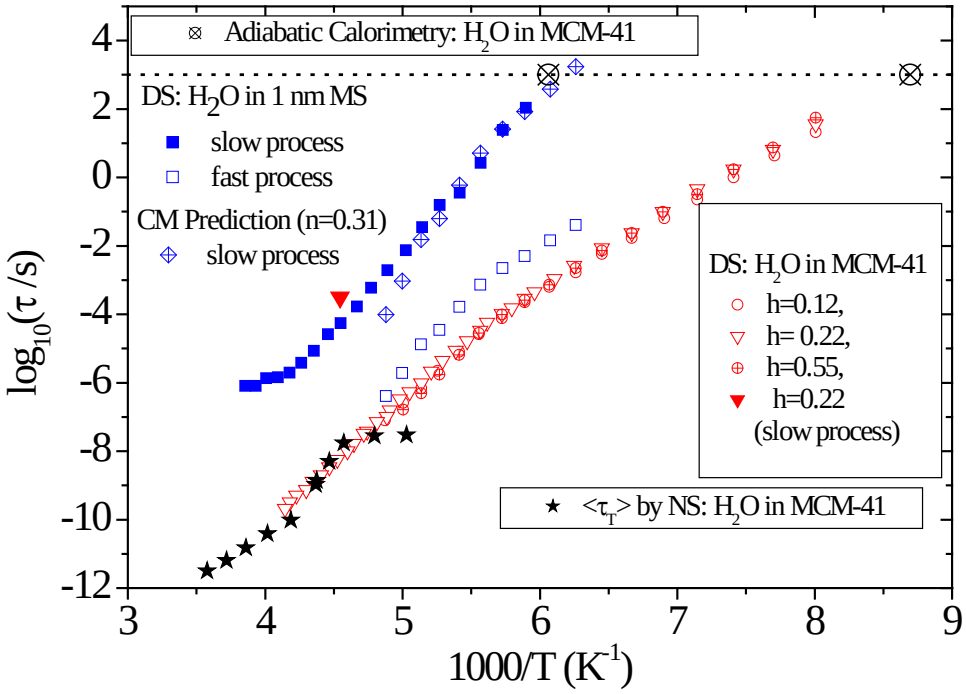

Figure 7. Plots of water relaxation times vs. reciprocal T for different confined systems. Blue solid and open squares: τ of slow and fast relaxation processes (respectively) of water confined in 10 Å molecular sieves obtained by dielectric spectroscopy [r055]. Crossed blue diamonds indicate the position of the slow process as predicted by CM (eq.1) with n=0.31. Dielectric data [r056] of τ_v of water confined in MCM-41 with pore diameter 2.14 nm at hydration levels h=0.12 (open circles), 0.22 (open triangles), 0.55 (open circles with + inside). The red solid triangle indicate relaxation time of slow process of water confined in MCM-41, h=0.22 [r056]. The two black crossed circles are relaxation time of slow and fast processes ($\tau=10^3$ s) of water confined within 1.2, 1.6 and 1.8 nm nano-pores of MCM-41 obtained by adiabatic calorimetry at T=115 and 165 K respectively [r015]. The black closed stars are translational relaxation time determined by neutron scattering of water confined in nanoporous MCM-41-S with pore diameters of 14 Å [r022].

Finally, a special comment should be devoted to the one of the most cited paper on the dynamics of nano-confined water, that is the study of water confined in nanoporous silica matrices MCM-41-S with pore diameters of 18 and 14 Å, by quasielastic neutron scattering [r058, r022]. The analysis, based on a relaxing cage model, determined the temperature variation of the average translational relaxation time $\langle\tau_T\rangle$ of water: a sharp change was found from VFTH-like at higher temperatures to Arrhenius law at T≈225 K with activation energies of 22.1 kJ/mol and 28.13 kJ/mol for 18 Å and 14 Å size pores respectively. This behaviour was interpreted as the fragile-to-strong liquid–liquid transition of water, involving $\langle\tau_T\rangle$ of the structural α-relaxation of nano-confined water. In Fig.7 we reported data for $\langle\tau_T\rangle$ for water

confined in MCM-41-S with pore diameters of 14 Å [r022]. A similar behaviour was observed in the T-dependence of the reciprocal of the self-diffusion NMR coefficient of water confined in the same system [r069]. Actually, as can be seen in Fig.7, the neutron $\langle\tau_T\rangle$ with the VFTH dependence are superposed to, and continue the trend of, the fast relaxation times of water confined in molecular sieves MCM-41 C10 with pore diameter 2.14 nm at hydration levels in the range h=0.12-0.55 obtained by dielectric spectroscopy [r056] and previously interpreted as primitive of JG-relaxation. Therefore we could infer that $\langle\tau_T\rangle$ obtained by the neutron scattering experiments is not the α-relaxation of supercooled water above 225 K, but instead the primitive or JG β-relaxation of water. Moreover, if we would try to extrapolate the Arrhenius T-dependence of the neutron $\langle\tau_T\rangle$ of Refs.[r022] and [r058] to temperatures below 225 K we would obtain glass transition temperatures (i.e. $\langle\tau_T\rangle = 10^2$-$10^3$ s) at very low values (less than 80 K), at odds with all literature data on glass-transition of supercooled water [r001]. Actually, the abrupt change of Arrhenius dependence observed at 225 K for $\langle\tau_T\rangle$ seems to not have any signature on dielectric data that, on the other hand, show a crossover at a lower T (near 166 K). The nature of the phenomenon observed from $\langle\tau_T\rangle$ in vicinity of 225 K deserves to be better investigated, but we can undoubtedly affirm that the measured neutron $\langle\tau_T\rangle$ for T <225 K are not connected to the α- relaxation of the supercooled confined water.

4. Dynamics of hydrated proteins

4.1 Hydrated Proteins and Biomolecules

From the previous sections, we have reviewed the dynamics of water seen in many different aqueous mixtures with hydrophilic solutes, and water in confinement. There are two major relaxation processes in aqueous mixtures. One is the relaxation originating from the water component in the aqueous mixtures, and the other is the structural relaxation of the solute hydrogen-bonded to the water. The properties of the two processes qualitatively are general and independent of the solute. Foremost is the symbiotic relation between the two relaxations, which indicates the participation of water in both processes. Changes of the two processes with content of water and molecular weight of solute conform to a regular pattern that can be rationalized from the degree of coupling of water to the solute and the molecular mobility of the neat solute or its T_g. The situation of hydrated proteins and biomolecules in general is different from aqueous mixtures. Only about two layers of water (called the hydration shell) surrounding the folded protein are of importance for the consideration of the dynamics responsible for full activation of the protein functionality [r070, r071]. From this, the dynamics of proteins is coupled to that of water or other solvents surrounding the protein molecules. However, in the literature, different views of this coupling and explanation of the dynamics have been offered [r010, r019, r035, r017, r071-r091].

Here we review some experimental data of hydrated biomolecules from dielectric relaxation, adiabatic calorimetry, and NMR to show the dynamics of water in the hydration shell and the hydrated biomolecule in essence are no different from the homogeneous aqueous mixtures and nano-confined water. Thus, we can transfer our understanding and interpretation of the dynamics of aqueous mixtures and nano-confined water in the previous sections to hydrated biomolecules. Historically, and continued to the present days, the study of dynamics of hydrated biomolecules are primarily spurred by Mössbauer spectroscopic and neutron scattering measurements of the mean square displacement (MSD), $\langle r^2\rangle$, of fast processes that can be observed within the time window typically shorter than the instrument resolution time, which is 140 ns for Mössbauer spectroscopy and 1 ns to 10 ps for various neutron scattering

measurements. In the past, the neutron scattering data of hydrated biomolecules were interpreted without the benefit of the knowledge gained using other techniques with longer time windows in the same systems or simpler systems of aqueous mixtures and confined water. By taking advantage of these other relevant experimental facts now available [r084, r085, r035, r019], a definitive interpretation of the Mössbauer spectroscopic and neutron scattering data can be given, which traces the so called 'dynamic transition' observed in the MSD to the dynamics of the primitive relaxation of hydration water or other solvents including aqueous mixtures and anhydrous hydrophilic substances. From the results and conclusions, the role of hydration water or other solvents for protein dynamics and function is given a new interpretation.

4.2 Dielectric relaxation and enthalpy relaxation experiments

The presence of bulk water in addition to hydration water in hydrated biomolecules makes the observed dynamics by dielectric relaxation [r035, r019, r086, r090, r091] and calorimetry [r084] more complicated than aqueous mixtures and confined water. Notwithstanding, these extraneous contributions were identified and separated out from the relevant structural relaxation of the hydrated biomolecule and the relaxation of water in the hydration shell. This has been done for the hydrated protein, 20% (w/w) aqueous solution of bovine serum albumin (BSA) studied by adiabatic calorimetry limited to long times of the order of 10^3 s, and by broadband dielectric measurements on the 20 and 40% (w/w) aqueous solution of BSA made over frequency range of twelve decades from 2 mHz to 20 GHz isothermally at temperatures from 80 K to 300 K. All processes observed were presented before [r035, r019]. Here the relaxation of ice formed in the bulk water is omitted for the sake of clarity in the discussion of the two major relaxation processes of water in the hydration shell and the hydrated. Their relaxation times determined from fits to the isothermal data of $\varepsilon^*(\nu)$ are plotted against reciprocal temperature in Fig.8.

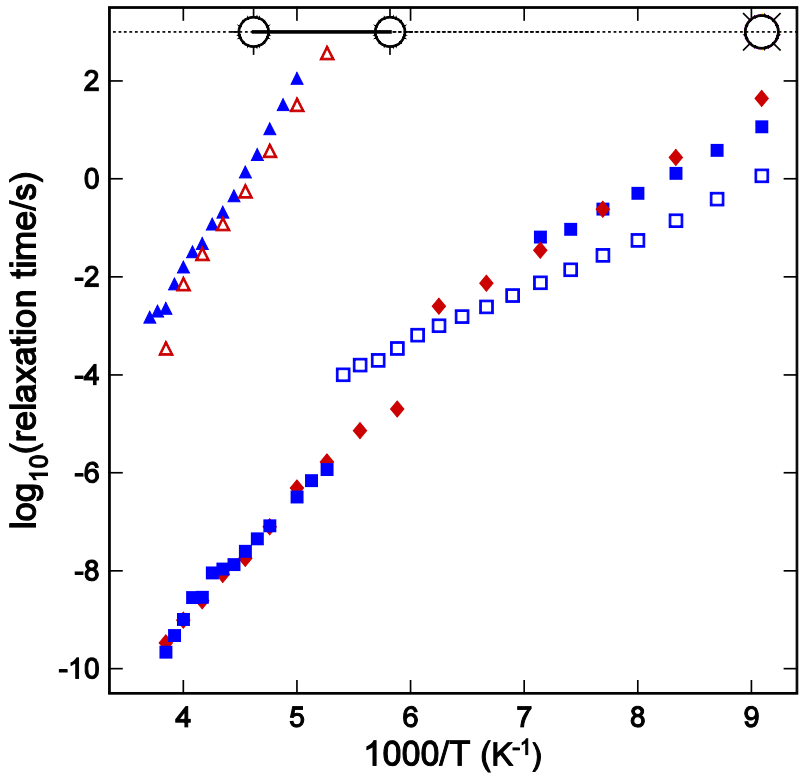

Figure 8. Dielectric relaxation times of 20 and 40% (w/w) solution of bovine serum albumin (BSA) in water

[r035]: The faster relaxation, with Arrhenius *T*-dependence below about 190 K and changing to a stronger *T*-dependence above it, is the β-relaxation of hydration water τ_W (squares for 20% and diamonds for 40%). The slower α-relaxation with relaxation times τ_{BSA} (triangles) reaches about 10^3 s at about 190 K. The two large circles joined by a line indicate the temperature range of the α-process of hydrated BSA and the large circle with four spokes is the temperature of the water β-relaxation observed by adiabatic calorimetry at 10^3 s [r084].

The loss peak of water in the hydration shell of the 20 wt% BSA-water mixture at lower temperatures is very broad and seems to be composed of two processes close to each other, and their relaxation times are represented by open and closed blue squares. A single process is obtained for the 40 wt% BSA-water mixture and shown by closed diamonds. All these relaxation times of water in the hydration shell, collectively denoted by τ_ν, have Arrhenius *T*-dependence from 100 K and up to about 200 K. Above 200 K, the relaxation times of water in the hydration shell are represented by blue open circles and closed diamonds for the 20 and 40% (w/w) BSA-water mixtures respectively. It can be seen that the Arrhenius *T*-dependence of τ_W at temperatures below about 200 K is replaced by a stronger and non-Arrhenius *T*-dependence after crossing some temperature in the neighborhood of 200 K. The gap between τ_W in this neighbourhood is the artifact of fitting isothermal data by Cole-Cole functions, and should not be there. The relaxation times of the hydrated BSA, τ_{BSA}, are shown by the blue closed triangles and brown open triangles for the 20 and 40% (w/w) BSA-water mixtures respectively. With the much stronger *T*-dependence, τ_{BSA} reaches the 10^2 to 10^3 s near 200 K, suggesting it is the structural α-relaxation and the glass transition of the hydrated BSA occurs at some temperature $T_{gBSA} \approx 200$ K. This happening is supported by heat capacity and enthalpy relaxation rate measurements of a 20 % (w/w) BSA-water mixture by Kawai et al. [r084]. These authors have found several enthalpy relaxations with relaxation time of 10^3 s originating from different processes. The one found in the broad range from 170 K to 220 K are indicated by the thick line at 10^3 s bounded on both sides by ⊗ in Fig.8. It can be seen from the figure that the dielectric τ_{BSA} falls within the temperatures range of enthalpy relaxation. Kawai et al. found another enthalpy relaxation with relaxation time of 10^3 s in the temperature range from 100 to 120 and centred at 110 K (indicated by ⊕). This temperature is in rough agreement with the dielectric τ_W when extrapolated to 10^3 s, proving that adiabatic calorimetry and dielectric relaxation are observing the same water relaxation. Almost the same enthalpy relaxation was found for water confined within 1.1, 1.6 and 1.8 nm nano-pores of silica MCM-41 [r015] and of silica gels [r013]. The τ_W of water in the hydration shell at temperature below T_{gBSA} is comparable in magnitude and activation energy to the dielectric JG relaxation of water in hydrophilic mixtures and nano-confined water [r008]. The change of the *T*-dependence of τ_W at T_{gBSA}, as well as the monotonic increase of its dielectric strength $\Delta\varepsilon_\nu$ with increasing temperature, is the same as those found for the same quantities of the ν-relaxation or the JG β-relaxation of water in other aqueous mixtures, nano-confined water, and a component in mixtures of two van der Waals glass-formers [r008]. All these properties of the water specific relaxation suggest that it is truly the primitive or JG relaxation of water in the hydration shell. This general relation between the JG β-relaxation and the α-relaxation has been explained by the Coupling Model [r010].

In Fig.9 we include data of the water-specific relaxation times τ_ν of other hydrated biomolecules for comparison with those of hydrated BSA. First are the dielectric and quasielastic neutron scattering data of lysozyme hydrated to a level of h=0.4 g water per gram of protein [r087-r090]. Second are the various relaxation time, τ_ν, of the hydration water in H_2O or D_2O-hydrated myoglobin (with hydration level in a range around 0.35 g/g) determined by deuteron NMR spectroscopy [r076], Mössbauer spectroscopy [r092], and neutron scattering [r080]. The deuteron NMR spectroscopy probes the reorientational relaxation of the O–D vector of the D_2O hydration water, and τ_ν obtained from about 200 to 300 K have been

fitted by the VFTH T-dependence, $\tau_v(T)=(0.96)\exp[460/(T\text{-}167)]$ ps, given in Ref.[r079]. Neutron scattering and Mössbauer spectroscopy obtain τ_v of hydrated myoglobin by either the observed from the dynamic transition exhibited by the mean square displacement [r092, r080]. Third are τ_v obtained from data analysis of neutron scattering from hydration water in hydrated c-phycocyanin (C-PC) [r093]. There is overall good agreement between τ_v determined by dielectric, NMR, Mössbauer spectroscopy, and neutron scattering in the four hydrated biomolecules having very different chemical and physical structures. What is common to the BSA, lysozyme, myoglobin and c-phycocyanin systems is the hydration water. According to our interpretation like in other non-aqueous and aqueous mixtures, and nano-confined water, the almost identical τ_v observed in the four hydrated biomolecules is the primitive or JG relaxation time of hydration water.

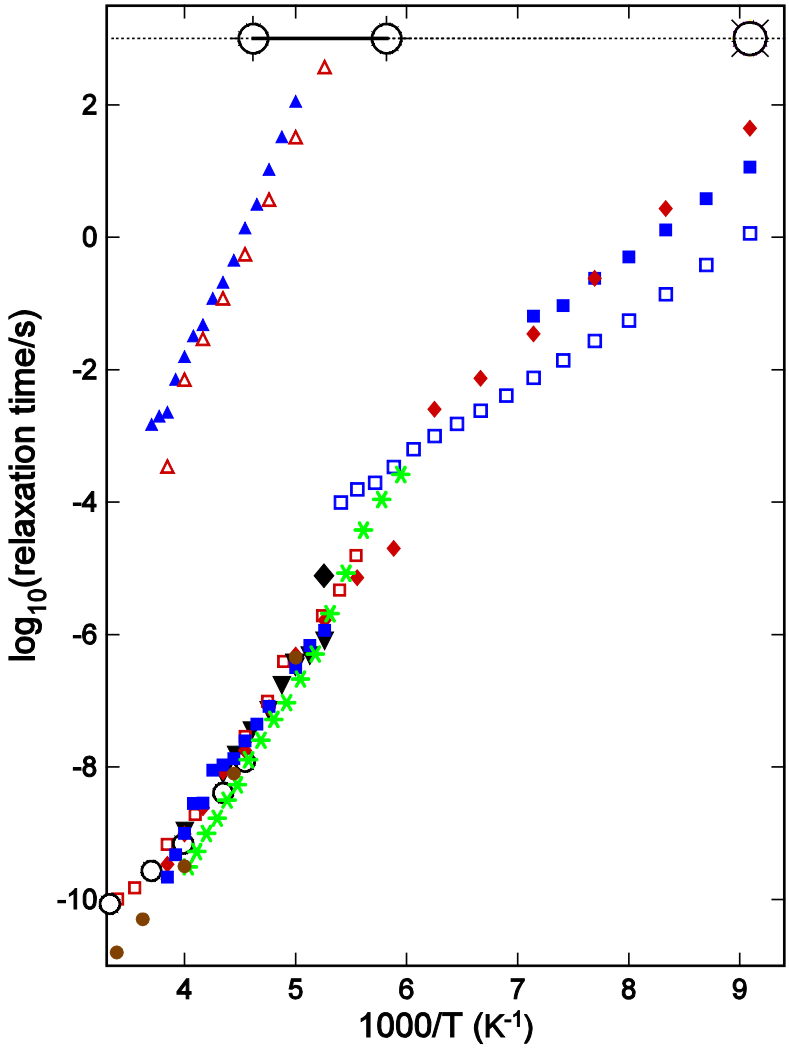

Figure 9. Dielectric data of hydration water in hydrated BSA same as in Fig.8. Added are the following data. The dielectric relaxation times, τ_{1K} (*), and neutron relaxation time (brown closed circles) of hydrated lysozyme by Khodadadi et al. [r088, r089, r090]. The relaxation times from neutron scattering (open black circles) [r080], from Mössbauer spectroscopy (black closed diamond) [r092], and τ_c from NMR (open red squares) [r076] of hydrated myoglobin. Relaxation times from neutron scattering from hydration water in hydrated c-phycocyanin (C-PC) (black closed triangles) [r093]. For relaxation times shorter than 10^{-6} s, all data of the hydration water relaxation times τ_v are practically overlapping each other, indicating that τ_v are approximately the same for four different hydrated biomolecules, BSA, lysozym, myoglobin, and c-phycocyanin.

As proven by the combination of dielectric relaxation and adiabatic calorimetry data of hydrated BSA in Fig.8, there are two distinctly different relaxations. The slower one is the cooperative relaxation of the biomolecule coupled together with the hydration water and has dielectric relaxation time τ_α reaching long time of the order of 10^3 s at the calorimetric glass transition temperature. The faster one is the water-specific relaxation which is not responsible for the glass transition. Nevertheless, its relaxation time τ_ν is sensitive to glass transition by the change of its *T*-dependence from Arrhenius law with activation energy of about 40-50 kJ/mol below T_g to stronger *T*-dependence above T_g. Like in hydrated BSA, the same two relaxations are found in hydrated myoglobin by dielectric relaxation [r094-r096] and the α-relaxation by low frequency heat capacity measurements and calorimetry (See the data labelled HW in Fig.3 of Ref.[r080]]. While we identify the relaxation times from neutron scattering, Mössbauer spectroscopy, and deuteron NMR spectroscopy with τ_ν, Doster considered them as τ_α and connect them with the relaxation times from heat capacity and calorimetry, which definitely are the cooperative α-relaxation times. After constructing this supposedly *T*-dependence of τ_α of hydration water and fitted it by the VFTH dependence (see Fig.3 of Ref.[r080]), the conclusion that water is a very fragile liquid was made. The conclusion is invalid because the relaxation times were taken from two distinct processes. This can be seen from the dielectric data of Swenson et al. [r094] that Doster took as τ_α of hydration water. He took only part of the relaxation times of the faster of the two processes at temperatures higher than about 182 K, and ignored the continuation of the data measured down to about 135 K with Arrhenius *T*-dependence. The mistake made in identifying the relaxation times from neutron scattering, Mössbauer spectroscopy, and deuteron NMR spectroscopy (as well as high frequency dielectric relaxation) as τ_α of hydration water is understandable because of the general lack of appreciation of the ubiquitous primitive or JG β-relaxation of water and the analogous behaviour found in the simpler systems of aqueous mixtures and nano-confined water. Also, based on short time neutron scattering data or deuteron NMR data alone, one can be led to the wrong identification of the relaxation processes without taking into consideration of the long time adiabatic calorimetric and dielectric relaxation data. Other researchers have made the mistake of identifying the relaxation times from neutron scattering and high frequency dielectric relaxation data with the α-relaxation of the protein. For example, Khodadadi et al. [r088, r089, r090] concluded their own data come from "structural relaxation of the protein" or "protein's structural relaxation coupled to hydration water". These authors honestly admitted of having difficulty to rationalize why, at the T_g~180 K, the relaxation time of this fast hydrated protein relaxation is ~10^{-4} to 10^{-5} s and not 10^2 or 10^3 s as expected for structural relaxation.

Quasielastic neutron scattering was used by H.-S. Chen et al. [r074] to determine of the average translational relaxation time, $\langle \tau_T \rangle$, for the hydration water in hydrated lysozyme at the hydration level of h = 0.3. The values of $\langle \tau_T \rangle$ they found that follow a VFTH *T*-dependence are nearly the same as those of other hydrated biomolecules presented in Fig.9, although not shown therein. However, the abrupt change of *T*-dependence of $\langle \tau_T \rangle$ to Arrhenius at temperatures below T_L=220 K they found and ascribed to fragile-to-strong transition of water was not seen by others in all hydrated biomolecules. Doster and co-workers have recently demonstrated this is an artefact, resulting from the procedure used to analyze the data [r093].

From the discussions above of the experimental data on dynamics of hydrated proteins, we conclude that the adiabatic calorimetric measurements [r084] are pivotal in proving that the two major relaxation processes, the primitive or ν-relaxation of hydration water and the structural α-relaxation, are distinct but yet connected. They are distinct because their relaxation times reach 10^3 s at vastly different temperatures, $T_{g\beta}$ for the β-relaxation and $T_{g\alpha}$ for the α-relaxation, determined by adiabatic calorimetry. They are connected because of the

observed change in the temperature dependence of the dielectric ν-relaxation time when $T_{g\alpha}$ is crossed. This relation is consistent with the simulations by Tarek and Tobias [r097] and by Wood et al. [r098], who found the protein structural relaxation are correlated with the protein-water hydrogen bond dynamics, and protein atomic fluctuations cannot occur without water translation in short time scale of the neutron scattering. These features are analogous to the dynamics found in many aqueous mixtures. Moreover, in the Arrhenius temperature regime, the β-relaxation time of hydration water in protein is comparable in magnitude and has similar activation enthalpy as the primitive or JG β-relaxation of many aqueous mixtures. There is also analogy with binary mixtures of van der Waals liquids, although the analogy is not total because in the absence of hydrogen bonding each component has its own α- and JG β-relaxations. There are other connections between the primitive or JG β-relaxation and the α-relaxation in mixtures and in neat glass-formers beyond the one discussed here. These connections occur because the primitive relaxation is the precursor of the many-body relaxation dynamics evolving with time until the α-relaxation is reached. The explanation has been given by the Coupling Model, and the same explanation applies to the dynamics of hydrated proteins.

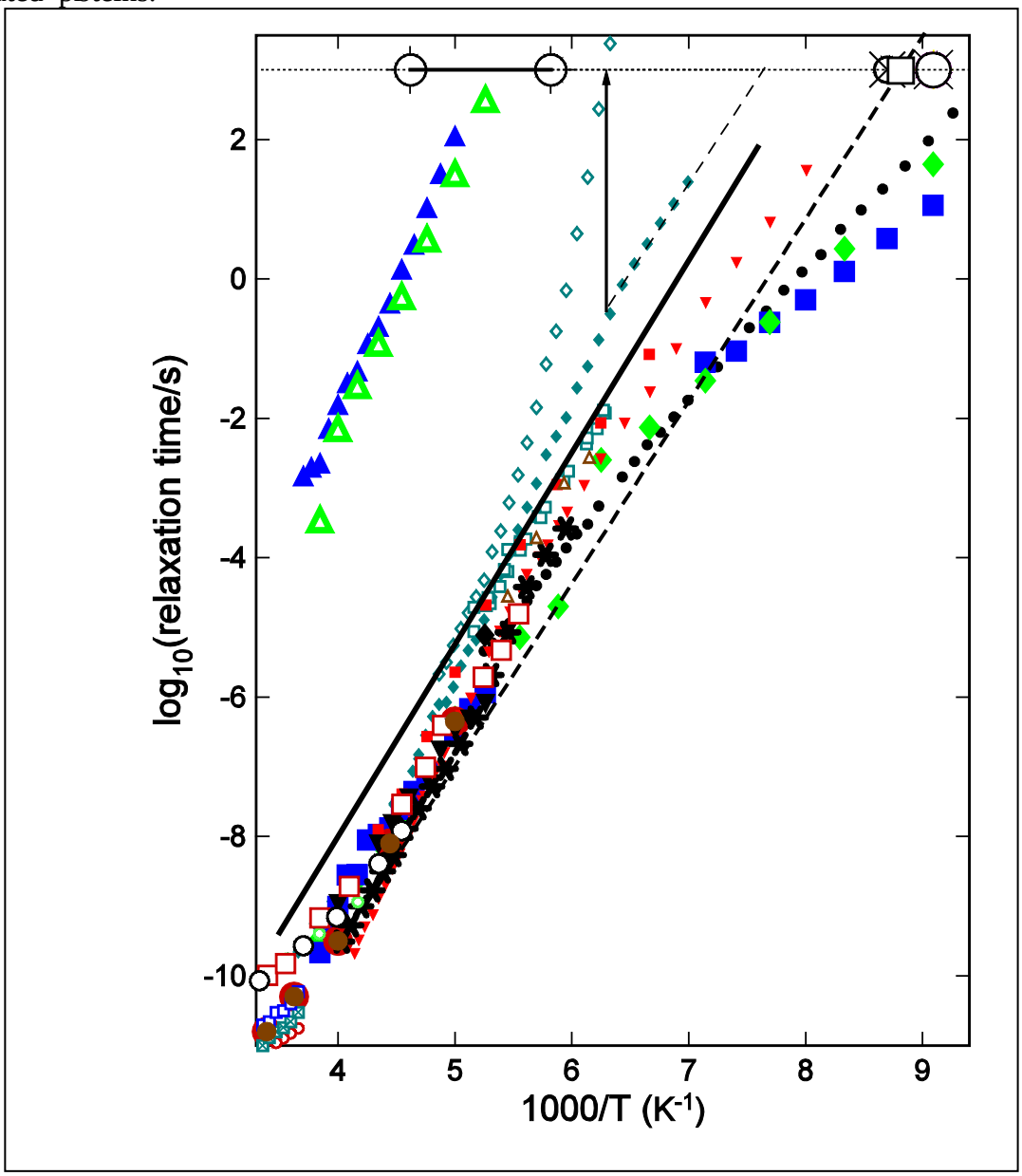

Figure 10. $\log_{10}(\tau)$ vs 1000/T. The larger symbols and are τ_α and τ_ν of the same hydrated biomolecules as

shown in Fig.9. The thick line is τ_v of hydrated collagen and elastin, as obtained from experimental data from ref.[r091]. All smaller symbols and thinner lines are for τ_{JG} or τ_v of aqueous mixtures and confined water. (1) 35 wt.% water mixture with 3EG (faint blue open diamonds for τ_α and closed diamond for τ_{JG}), 50 wt.% water mixture with PVME (red closed squares), 50 wt.% water with PVP (blue open square) [r099], 38.6 wt % of water with PHEMA (brown open triangles) [r062, r063], 20 wt.% water with 1-propanol (black •) [r008]. At times shorter than 10^{-10}s are τ_v of 90 wt % water with poly(vinyl alcohol) (pale blue squares with × inside), 80 wt.% water with PVP at short times (blue open squares) [r100], and bulk water at short times (brown open circles [r101]). The long thinner dashed line is the Arrhenius fit to τ_v of 20% of water nano-confined in graphite oxide from dielectric relaxation, actual data not shown [r068], and green open circles with $\tau_{JG} < 10^{-9}$s are from neutron scattering [r102, r103]). Dielectric data of relaxation time of water confined in MCM-41 with pore diameter 2.14 nm at hydration levels of 22 wt% (green▼). The horizontal dashed line indicate $\tau_v=10^{-9}$ s, the upper bound of the time window of neutron scattering instrument having energy resolution of 1 μeV.

The most convincing way we can demonstrate that the fast water specific relaxation observed in hydrated biomolecules is the primitive relaxation of water is to compare their relaxation times τ_v shown before in Figs.8 and 9 with the primitive or JG β-relaxation times of the water component in several aqueous mixtures and water nano-confined. All data of τ_v of hydrated biomolecules are shown now in Fig.10 by large symbols to distinguish them from those of τ_v of water in various mixtures and in confinement. Added are the data of τ_v found in hydrated collagen and elastin [r091], shown here by the thick line with Arrhenius temperature dependence in the temperature range faithfully reproduced. The adiabatic calorimetry data of water confined in molecular sieves and silica gels are added to the hydrated BSA data on the line with $\log(\tau/\mathrm{s})=3$. The small open and closed pale blue diamonds are τ_α and τ_v of 35 wt% of water mixture with tri-ethylene glycol, and are shown here to reemphasize the generally observed change of T-dependence of τ_v at T_g of aqueous mixtures including the hydrated BSA, myoglobin, and lysozyme. The solutes in the aqueous mixtures include poly(vinylpyrrolidone), PEHMA, PVME, PVA, PEG, PEI, and 1-propanol, and water confined in MCM-41 and graphite oxide [r068]. High frequency dielectric data of bulk water is also included in the plot. We can see that τ_v of the water specific process in hydrated biomolecules when it becomes short ($< 10^4$ s in the examples here) is nearly indistinguishable from τ_{JG} of aqueous mixtures and confined water. At low temperatures in the glassy state, the deviations of dielectric τ_v of water in hydrated BSA from τ_v is noteworthy but probably due to large uncertainty in determining τ_v from the very broad loss peaks [r035]. Nevertheless, the adiabatic τ_v of hydrated BSA is in good agreement with some average of τ_v from aqueous mixtures and confined water.

By inspection of Fig.10, we can see that there is no substantial difference between τ_v of hydration water of biomolecules and τ_v of aqueous mixtures, nano-confined water, and even bulk water when the relaxation times are short enough. Thus, we can confidently conclude that the primitive relaxation of hydration water is responsible for the observed process in neutron scattering, Mössbauer spectroscopy, and deuteron NMR spectroscopy.

4.3 Origin of the dynamic transition observed in neutron scattering experiments

The time scales of the MSD measured by neutron scattering depend on the energy resolution of the instrument. Roughly, instrument energy resolution 1 μeV corresponds to time scale of 1 ns. On increasing temperature, the measured MSD exhibits a change from weaker temperature dependence to a significantly stronger dependence at some temperature, T_D, traditionally referred to as the dynamic transition temperature. The temperature T_D is dependent on the protein, the solvent and its weight fraction. Neutron scattering measurements of myoglobin hydrated by fully deuterated water show the same characteristic temperature dependence of

the MSD and the same T_D, and this result indicates that the non-exchangeable hydrogens of the hydrated protein participate in the motions from which the observed dynamic transition of MSD originates. Examples can be taken from the paper by Tsai et al. [r081] of four samples prepared to maximize the scattering from the protein relative to the other components, and recent work by Wood et al. [r098]. This finding is consistent with the coupling of the water-specific relaxation to the motion of hydrogen atoms of the biomolecules as concluded before for aqueous mixtures from the dependence of τ_ν on composition and the solute in Section 3.

The phenomenon was first interpreted by Doster and coworkers [r077] as a "dynamic transition" of protein motions, which are coupled to the kinetic glass transition of the solvent near the protein surface. This interpretation was made more explicit by Doster [r079] by that the statement: "water near the protein surface can perform long range diffusion, which is arrested near 200 K [r078], it shows liquid behaviour above 200 K and glassy behaviour below. The slow α-process can be associated with the elementary step of diffusion. Hydration- and bulk water thus differ essentially in the magnitude of the diffusion coefficient and the rate of crystallization.". A more recent view is given essentially by Fig.3 in Ref.[r080].

A different interpretation of such a rapid increase in the conformational MSD was given by Frauenfelder and coworkers [r072, r073, r075, r017]. These authors suggested from their energy landscape model of hydrated proteins with hierarchical tiers that it is due to the β-fluctuations (in the hydration shell) in the lowest tier, which has Arrhenius temperature dependence for its relaxation time.

Sokolov and coworkers [r087] argued, from their dielectric and neutron data of lysozyme at hydration level of h=0.4, that this process is a coupled protein-solvent structural relaxation.

Zanotti et al. [r083] believed that the rapid increase of MSD is not associated with a thermal event as detected by calorimetry and suggested that it is more appropriate to describe the phenomenon as "dynamic crossover" instead of "dynamic transition". Actually, the first explanation of the protein "dynamic transition" as a dynamic phenomenon entering the time-scale of the spectrometer was given by Daniel and co-workers [r119].

Here we show that the primitive or JG β-relaxation of water, or solvent in general, is actually responsible for the observation of the dynamic transition in $<r^2>$ by neutron scattering. It has nothing to do with the structural relaxation and the glass transition of the hydrated biomolecule, consistent with Zanotti et al. [r083] that the dynamic transition is not associated with a thermal event. On increasing temperature, the sharp rise of $<r^2>$ starting at T_D is caused by a hydration-induced fast relaxation process that begins to enter into the short time window of the neutron spectrometer [r104, r105]. By inspection of the relaxation map of Figs.8-10, the fast true relaxation process first entering the time window of the neutron spectrometer is definitely the primitive or ν-relaxation of hydration water. Although this conclusion is obvious, we strengthen it by comparing what we expect from the ν-relaxation with experiments published in the literature.

Firstly, as shown in Fig.10, τ_ν is nearly independent of the hydrated biomolecule in the time range from 10 ps to 1 ns probed by using various neutron scattering spectrometers with different energy resolutions. From this, if the dynamic transition originates from ν-relaxation entering the time window of the spectrometer, we expect that the dynamic transition temperature T_D is nearly the same for different hydrated biomolecule when measured by spectrometers having the same resolution.

IN16 at ILL as well as the back-scattering spectrometer instrument at NIST have an energy resolution of about 1 μeV with corresponding time window t_{exp} of about 1 ns. In fact measurements using IN6 of hydrated Human serum butyrylcholinesterase (HuBChE) including HuBChE-H_2O and HuBChE-D_2O [r105], Wild-type (WT), the AA, and AA+Y RC mutants from R. sphaeroides, [r106], maltose binding protein samples, H-MBP-D_2O and D-

MBP-H_2O [r098], and 0.4 gD_2O g^{-1} hydrated lysozyme [r083], as well as measurements of lysozyme and RNA hydrated by D_2O [r087, r088, r081, r089] using the NIST spectrometer all have nearly the same T_D in the range of 220 to 225 K. Moreover, at these temperatures, the relaxation time of the hydration water τ_ν matches the time scale of the IN16 spectrometer t_{exp} of the order of ns, as can be verified by inspection of Fig.9 or 10.

IN13 at ILL has energy resolution (FWHM) of 8 μeV, which gives access to dynamics on a time scale above 150 ps and up to 400 ps. Approximately the same T_D from 225-240 K were reported the following studies using IN13. (1) D_2O hydrated myoglobin by Doster et al. [r077], (2) C-phycocyanin (C-PC) by Köper et al. [r107], (3) various deuterated sucrose/water and trehalose/water mixtures by Magazú et al. [r108], (4) hydrated single-stranded and double-stranded DNA [r109], and (5) ferric horse myoglobin (met–Mb) hydrated with D_2O at 20% level [r110].

IN6 at ILL has energy resolution of 90 μeV corresponding to t_{exp} of 10 ps. The T_D of hydrated heparan sulphate (HS-0.43 g/g) measured by this spectrometer is about 255 – 260 K [r105]. The Fermi Chopper spectrometer at NIST has comparable resolution of 140 μeV and T_D of the 24 wt% hydrated ribonuclease (RNase) measured by this spectrometer [r111]. Despite the difference between the two biomolecules, T_D is about 260 K, the same for both HS-0.43 g/g and the hydrated RNase. It can be seen from Figs. 9 or 10 at T=260 K, the ν-relaxation time of the hydration water τ_ν starts to become comparable to the 10 ps time scale t_{exp} of these spectrometers.

The time scale t_{exp} of Mössbauer spectroscopy is 140 ns. The classic experiment of Parak et al. on deoxy-myoglobin crystals using this techniques found T_D≈200 K [r092]. From Figs. 9 or 10, one can verify that τ_ν is comparable with 10^{-7} s at 200 K, which again is consistent with t_{exp} =140 ns of Mössbauer spectroscopy.

So far we have discussed biomolecules hydrated by pure water. Neutron scattering data of dynamic transitions exists in biomolecules when the solvent is not water or mixtures of water with hydrophilic solutes. Because of space limitation, the following results will be stated without supporting material. If the solvent is not water like glycerol [r081], it is the primitive or JG β-relaxation of glycerol that is responsible for the dynamic transition observed. If the solvent is aqueous mixtures such as 80% sucrose-water [r112, r113, r080], it is the water-specific secondary relaxation of the mixture of 80% sucrose-water (like that present in all aqueous mixtures as shown in Section 3) that triggers the dynamic transition as observed by Mössbauer spectroscopy [r112, r080]. At T_D≈230 K, the viscosity of the solvent is 6.4×10^{11} poise which is equivalent to the α-relaxation. In the case that the solvent is 90% or 25% glycerol-water, it can be seen from Fig.4 that the water-specific secondary relaxation has merged with the α-relaxation already at temperatures lower than T_D=210 K of Mössbauer spectroscopy at 140 ns and higher T_D of neutron scattering at times shorter than 1 ns. Usually after the secondary and the primary relaxations have merged, the cooperativity is much reduced and the merged relaxation is more like the secondary relaxation [r114].

To further show the relation of the secondary relaxation of the solvent to the dynamic transition, the neutron scattering MSD data of dry trehalose-coated carbon monoxy myoglobin (CO-myoglobin) obtained by Cordone et al. using IN6 [r115] is compared with the MSD data of protein C-phycocyanin (C-PC) hydrated by D_2O with h=0.5, and by D_2O with various deuterated trehalose by Köper et al. using IN13 [r107] in order to observe individual motions of the non-exchangeable protons of the protein. These include the C-PC/trehalose/D_2O samples with compositions 1.0/0.3/0.7, 1.0/0.75/0.75, and 1.0/1.0/0.0. The last one is entirely deuterated trehalose. No dynamic transition was observed for trehalose, and the MSD and the density of state function are those of a harmonic solid, up to room temperature in the case of CO-myoglobin, and up to above 320 K in the case of C-CP. No dynamical transition was observed, in contrast to proteins hydrated by D_2O. This can be

explained by the γ-relaxation times of trehalose, τ_γ, is still longer than 1 ns and the JG β-relaxation time, τ_β, is much longer than 1 ns at 320 K, compared with the time window of 15 ps for IN6 and 400 ps for IN13. These can be seen by inspection of the relaxation map of trehalose given in Ref.[r116]. Since the motion associated with the intramolecular γ-relaxation and the intermolecular JG β-relaxation do not occur in the neutron scattering temperature range, it is clear no dynamic transition from protein fluctuations can be observed in the protein/trehalose samples even the protein is coupled to the trehalose via hydrogen bonding. This also explains on a molecular dynamics basis the role of trehalose in stabilizing protein by inhibiting some of its fluctuations which cause protein unfolding and denaturation. Our explanation based on the secondary relaxations of trehalose is more directly related to experiment than those based on the ''high viscosity'' hypothesis, according to which the denaturation processes are hindered by the higher glass transition temperature of trehalose solutions [r117, r118], at least as far as connection with the dynamic transition is concerned. This is because viscosity is related to the structural α-relaxation of trehalose, which definitely is not involved in causing the dynamic transition.

5. Conclusion

The water-specific ν-relaxation is ubiquitous in aqueous mixtures, confined water, and hydrated biomolecules. Its presence is accompanied by the cooperative α-relaxation in aqueous mixtures and hydrated biomolecules, and the two relaxations are connected as shown by interrelations of their properties in several ways. The interrelations are the same as found in binary mixtures of van der Waals glass-formers, except for some variations caused by the prevalence of hydrogen bondings and the small size of the water molecule compared with other glass-formers. These include the change of the *T*-dependence of τ_ν from Arrhenius below T_g to a stronger *T*-dependence above T_g. The dielectric strength of the ν-relaxation increases monotonically with temperature, and it also assumes a stronger *T*-dependence above T_g. Thus, the water-specific ν-relaxation is the precursor of the α-relaxation, the same fundamental role played by the primitive or Johari-Goldstein β-relaxation of glass-formers in general in accordance with the Coupling Model interpretation. Utilizing the observed general properties of the water-specific ν-relaxation, we have ruled out the interpretations by others of this process as either the α-relaxation or the merged α- and β-relaxation of water at temperatures above T_g of the mixture and is transformed to local secondary relaxation of water by spatial confinement in the glassy state.

The relaxation time τ_ν of the water-specific ν-relaxation in the glassy state of the aqueous mixtures and hydrated biomolecules assumes the nearly universal Arrhenius *T*-dependence independent of the solute wherever the molar fraction of water in the mixture is sufficiently high. This common *T*-dependence of τ_ν of aqueous mixtures is approximately the same as the relaxation of water confined in nano-meter space. The activation energy is about 50 kJ/mol, the energy needed to break two hydrogen bonds to allow water molecules to rotate and translate. The stronger *T*-dependence of τ_ν in the liquid state after crossing T_g becomes milder at higher temperatures. Eventually, at temperatures sufficiently high above T_g, the *T*-dependences of τ_ν of aqueous mixtures and hydrated biomolecules all return to assume the temperature dependence close to the near universal Arrhenius *T*-dependence established in the glassy state and extrapolated to high temperatures. In the ideal case that the T_g of the aqueous mixture or hydrated biomolecule is very high, the near universal Arrhenius *T*-dependence of the glassy state will be observed over more than ten decades of τ_ν, say from 10^3 s to 10^{-9} s. This scenario is realized in hydrated collagen and elastin, and water confined in graphite

oxide as shown in Fig.10. These remarkable experimental facts which are independent of the solute in aqueous mixtures, the protein in hydrated proteins, and the method in confinement of water suggest water itself has low intermolecular cooperativity and its relaxation time would be close to Arrhenius had crystallization not pre-empted the study of its dynamics over the entire range of temperature.

On the dynamics transition of hydrated biomolecules, we have confirmed, as pointed out previously [r119], that the dynamics transition temperature T_D depends only on the time scale t_{exp} of the spectrometer, but we demonstrated that T_D does not depend on the biomolecule when it is hydrated sufficiently. This fact alone suggests that the ν-relaxation of the hydration water coupled with the hydrated biomolecule is responsible for the occurrence of the dynamic transition. This is because τ_ν is independent of the biomolecule within the time windows of Mössbauer spectroscopy and neutron scattering as shown in Figs. 9 and 10. Furthermore, as a quantitative proof, the observed T_D is in good agreement with that obtained by matching $\tau_\nu(T_D)$ with t_{exp}. These findings establish without doubt that the water-specific ν-relaxation coupled to the hydrated biomolecule is responsible for the dynamic transition. The importance of role played by the water-specific ν-relaxation in instability of the hydrated proteins becomes clear since the dynamic transition is an indicator of the onset of instability.

Acknowledgement
The work was supported at NRL by the Office of Naval Research. S.A. acknowledges the support of Galilei Ph.D. School.

References

[r001] P.G. Debenedetti, J. Phys. Condens. Matter, 15 R1669 (2003)
[r002] CA Angell, Supercooled water. Water: A Comprehensive Treatise, ed Franks F (Plenum, New York), Vol 7 (2008) 1–81
[r003] D. Bertolini, M. Cassettari, G. Salvetti, J. Chem. Phys. 76 (1982) 3285
[r004] C. Rønne, PO Åstrand, SR Keidung, J. Chem. Phys., 107 (1997) 5319
[r005] C. Masciovecchio, SC Santucci, A Gessini, S Di Fonzo, G Ruocco, F Sette, Phys. Rev. Lett. 92 (2004) 255507
[r006] G.P. Johari, A. Hallbrucker, E. Mayer, Nature 330 (1987) 552
[r007] O. Mishima, HE Stanley, Nature 396 (1998) 334
[r008] S. Capaccioli, K. L. Ngai, N. Shinyashiki, J. Phys. Chem. B 111 (2007) 8197
[r009] S. Cerveny, A. Alegria, J. Colmenero, Phys. Rev. E 77 (2008) 031803
[r010] K.L. Ngai, S.Capaccioli, N. Shinyashiki, J.Phys.Chem.B 112 (2008) 3826
[r011] S. Mashimo, S. Kuwabara, S. Yagihara, K. Higasi, J. Phys. Chem. 91 (1987) 6337
[r012] P. Mazur, Science 168 (1970) 939
[r013] M. Oguni, S. Maruyama, K. Wakabayashi, A. Nagoe, Chem. Asian J. 2 (2007) 514
[r014] E. Tombari, G. Salvetti, C. Ferrari, G.P. Johari, J. Chem. Phys. 122 (2005) 104712
[r015] M. Oguni, Y. Kanke, and S. Namba, AIP Conf. Proc. 982 (2008) 34
[r016] K. Hofer, E. Mayer, G.P. Johari, J. Phys. Chem., 94 (1990) 2689; 95 (1991) 7100
[r017] H. Frauenfelder, G. Chen, J. Berendzen, P. W. Fenimore, H. Jansson, B. H. McMahon, I. R. Stroe, J. Swenson, R. D. Young, Proc. Natl.Acad. Sci. USA, 106 (2009) 5129.
[r018] J. Swenson, H. Jansson, R. Bergman, Phys. Rev. Lett., 96, 247802 (2006)
[r019] K. L. Ngai, S. Capaccioli, M. Shahin Thayyil, N. Shinyashiki, J Therm Anal Calorim 99 (2010)123–138

[r020] N. Shinyashiki, S. Sudo, S. Yagihara, A. Spanoudaki, A. Kyritsis, P. Pissis, J. Phys.: Condens. Matter 19 (2007) 205113.
[r021] S. Cerveny, G.A. Schwartz, A. Alegria, R. Bergman, J. Swenson, J. Chem. Phys. 124 (2006) 194501.
[r022] L. Liu, S.-H. Chen, A. Faraone, C.-W.Yen, C.-Y. Mou, Phys. Rev. Lett. 95 (2005) 117802
[r023] S. Cerveny, J. Colmenero, and A. Alegría, Phys. Rev. Lett. 97 (2006) 189802
[r024] J. Swenson, Phys. Rev. Lett. 97 (2006) 189801
[r025] S. Cerveny, G. Schwartz, R. Bergman, J. Swenson, Phys. Rev. Lett. 93 (2004) 245702.
[r026] G.P. Johari, M. Goldstein, J. Chem. Phys. 53 (1970) 2372.
[r027] K. Kessairi, S. Capaccioli, D. Prevosto, M. Lucchesi, S. Sharifi, PA Rolla, J. Phys. Chem. B 112 (2008) 4470-4473.
[r028] K.L. Ngai, J. Phys.: Condens. Matter**,** 15 (2003) S1107.
[r029] K.L. Ngai, M. Paluch, J. Chem. Phys. 120 (2004) 857.
[r030] *n* can be estimated from the dispersion of the α-relaxation only when other sources of broadening, like fluctuation concentration, are negligible.
[r031] S. Sudo, M. Shimomura, T. Saito, T. Kashiwagi, N.Shinyashiki, S.Yagihara, J. Non-Cryst.Solids 305 (2002) 197.
[r032] S. Sudo, M. Shimomura, K. Kanari, N. Shinyashiki, S. Yagihara, J. Chem. Phys. 124 (2006) 044901.
[r033] S. Sudo, S. Tsubotani, M. Shimomura, N. Shinyashiki, S. Yagihara, J. Chem. Phys. 121 (2004) 7332.
[r034] K. Grzybowska, M. Paluch, A. Grzybowski, S. Pawlus, S. Ancherbak, D. Prevosto, S. Capaccioli, J. Phys. Chem. Lett. 1 (2010) 1170
[r035] N. Shinyashiki, W. Yamamoto, A.Yokoyama, T.Yoshinari, S.Yagihara, R. Kita, K. L. Ngai, S. Capaccioli, J. Phys. Chem. B 113 (2009) 14448–14456
[r036] A. Doss, M. Paluch, H. Sillescu and G. Hinze, J. Chem. Phys., 117 (2002) 6582
[r037] M. Mierzwa, S. Pawlus, E. Kaminska, M. Paluch and K.L. Ngai, J.Chem.Phys. 128 (2008) 044512.
[r038] T. Blochowicz, E.A. Roessler, Phys. Rev. Lett. 92 (2004) 225701.
[r039] S. Capaccioli, K. Kessairi, D. Prevosto, M. Lucchesi, P. Rolla, J. Phys.: Condens. Matter 19 (2007) 205133.
[r040] S. E. Pagnotta, S. Cerveny, A. Alegría, J. Colmenero, J. Chem. Phys. 131 (2009) 085102
[r041] A. Schönhals, H. Goering, Ch. Schick, B. Frick, R. Zorn, J. Non-Cryst.Solids 351 (2005) 2668.
[r042] M. Paluch, C.M. Roland, S. Pawlus, J. Ziolo. K.L. Ngai, Phys. Rev. Lett. 91 (2003) 115701.
[r043] R. Bergman, F. Alvarez, A. Alegrıa, and J. Colmenero, J Chem. Phys. 109 (1998) 7546
[r044] R. Bergman and C. Svanberg, Phys. Rev. E 72 (2005) 043501
[r045] A. Nowaczyk, B.Geil, G.Hinze, R.Böhmer, Phys.Rev.E 74 (2006) 041505.
[r046] K.L. Ngai, J. Chem. Phys. 109 (1998) 6982
[r047] P. Kumar, G. Franzese, H.E. Stanley, Phys. Rev. Lett., 100 (2008) 105701
[r048] M. Vogel, Phys. Rev. Lett., 101 (2008) 225701
[r049] A. Schönhals, F. Kremer, A. Hofmann, E.W. Fischer, E. Schlosser, Phys. Rev. Lett. 70 (1993) 3459
[r050] K. Grzybowska, A. Grzybowski, J. Zioło, M. Paluch, S. Capaccioli, J. Chem. Phys. 125 (2006) 044904
[r051] R. Bergman, J. Swenson, Nature 403 (2000) 283.
[r052] R. Bergman, J. Swenson, L. Borjesson, P. Jacobsson, J. Chem. Phys. 113 (2000) 357.

[r053] S. Capaccioli, K. L. Ngai, J.Phys.Chem.B 109 (2005) 9727.
[r054] R. Bohmer, K.L. Ngai, C.A. Angell, D.J. Plazek, J. Chem. Phys. 99 (1993) 4201.
[r055] H. Jansson, J. Swenson, Eur. Phys. J. E 12 (2003) S51.
[r056] J. Hedström, J.Swenson, R. Bergman, H. Jansson, S. Kittaka Eur. Phys. J. Special Topics 141 (2007) 53-56.
[r057] J. Swenson, H. Jansson, WS. Howells, S. Longeville, J.Chem.Phys. 122 (2005) 084505.
[r058] A. Faraone, L. Liu, C.-Y. Mou, C.-W. Yen, S.-H. Chen, J. Chem.Phys. 121 (2004) 10843
[r059] M. Cammarata, M. Levantino, A. Cupane, A. Longo, A. Martorana, F. Bruni, Eur. Phys. J. E 12 (2003) S63.
[r060] A. Cupane, M. Levantino, M.G. Santangelo, J. Phys. Chem. B 106 (2002) 11323.
[r061] G. Schirò, A. Cupane, S.E. Pagnotta, F. Bruni, J. Non-Cryst. Solids 353 (2007) 4546.
[r062] K. Pathmanathan, G. P. Johari, J. Polym. Sci. Polym. Phys. B 28 (1990) 675.
[r063] K. Pathmanathan, G.P. Johari, J. Chem. Soc. Faraday Trans. 90 (1994) 1143.
[r064] G.P. Johari, J. Chem. Phys. 105 (1996) 7079.
[r065] L. Bosio, G.P. Johari, M. Oumezzine, J. Teixeira, Chem. Phys. Lett. 188 (1992) 113.
[r066] W. A. Kamitakahara, N. Wada, Phys. Rev. E. 77 (2008) 041503
[r067] V.Crupi, D. Majolino, V.Venuti, J. Phys.: Cond. Matter 16 (2004) S5297
[r068] S. Cerveny, F. Barroso-Bujans, A. Alegria, J. Colmenero, J. Phys. Chem. B, 114, (2010) 2604
[r069] F. Mallamace, M. Broccio, C. Corsaro, A. Faraone, U. Wanderlingh, L. Liu, C.-Y. Mou, S.-H. Chen, J. Chem. Phys. 124 (2006) 161102.
[r070] R. B. Gregory, editor "*Protein-solvent interactions,*" Marcel Dekker, New York (1995).
[r071] D. Ringe, G. A. Petsko, Biophys. Chem. 105 (2003) 667.
[r072] P.W. Fenimore, H. Frauenfelder, B.H. McMahon, F.G. Parak, Proc.Natl. Acad. Sci. U.S.A. 99 (2002) 16047.
[r073] P. Fenimore, H. Frauenfelder, B. McMahon, R.D. Young, Proc.Nat.Acad.Sci. 101, (2005) 14408.
[r074] S.-H. Chen, L. Liu, E. Fratini, P. Baglioni, A. Faraone, and E. Mamontov, Proc. Natl. Acad. Sci. U.S.A. 103 (2006) 9012.
[r075] G. Chen, P. W. Fenimore, H. Frauenfelder, F. Mezei, J. Swenson, R. D. Young, Philos. Mag., 88 (2008) 3877.
[r076] S.A. Lusceac, M.R. Vogel, C.R. Herbers, Biochimica et Biophysica Acta 1804 (2010) 41.
[r077] W. Doster, S. Cusak, W. Petry, Nature, 337 (1989) 754.
[r078] W. Doster, M. Settles, Biochim. Biophys. Acta, 1749 (2005) 173.
[r079] W. Doster, Eur. Biophys. J. 37 (2008) 591.
[r080] W. Doster, Biochimica et Biophysica Acta- Proteins and Proteomics 1804 (2010) 3.
[r081] A. M. Tsai, D. A. Neumann, L. N. Bell, Biophys. J., 79 (2000) 2728.
[r082] A. Paciaroni, S. Cinellli, G. Onori, Biophys. J., 83 (2002) 1157.
[r083] J.-M. Zanotti, G. Gibrat, M.-C. Bellissent-Funel, Phys.Chem. Chem. Phys., 10 (2008) 4865.
[r084] K. Kawai K., T. Suzuki, M. Oguni, Biophys. J. 90 (2006) 3732.
[r085] J. Swenson, H. Jansson, J. Hedström, R. Bergman, J. Phys., Condens. Matter 19 (2007) 205109.
[r086] K. L. Ngai, S. Capaccioli, N. Shinyashiki, M. Shahin Thayyil, J. Non-Cryst. Solids 356 (2010) 535.
[r087] S. Khodadadi, A. Malkovskiy, A. Kisliuk, A.P. Sokolov, Biochimica et Biophysica Acta-Proteins and Proteomics 1804 (2010) 15.

[r088] S. Khodadadi, S. Pawlus, J.H. Roh, V. Garcia Sakai, E. Mamontov, A.P. Sokolov, J. Chem. Phys. 128 (2008) 195106.
[r089] A.P. Sokolov, J.H. Roh, E. Mamontov, V. Garcia Sakai, Chem. Phys. 345 (2008) 212.
[r090] S. Khodadadi, S. Pawlus, A.P. Sokolov, J. Phys. Chem. B 112 (2008) 14273.
[r091] C. Gainaru, A. Fillmer, R. Böhmer, J. Phys. Chem. B, 113 (2009) 12628.
[r092] F. Parak, E. W. Knapp, D. Kucheida, J. Mol. Biol., 161 (1982) 177.
[r093] W. Doster, S. Busch, A. M. Gaspar, M.-S. Appavou, J. Wuttke, H. Scheer, Phys. Rev. Lett. 104 (2010) 098101.
[r094] J. Swenson, H. Jansson, R. Bergman, Phys. Rev. Lett. 96 (2006) 247802.
[r095] H. Jansson, R. Bergman, J. Swenson, J. Phys. Chem. B 109 (2005) 24134.
[r096] H. Jansson, J. Swenson, Biochimica et Biophysica Acta 1804 (2010) 20.
[r097] M. Tarek, D.J. Tobias, Phys. Rev. Lett. 88 (2002) 138101.
[r098] K. Wood, A. Frölich, A. Paciaroni, M. Moulin, M. Hartlein, G. Zaccai, D. J. Tobias, M. Weik, J.Am.Chem.Soc. 130 (2008) 4586.
[r099] S.K. Jain, G.P. Johari, J. Phys. Chem., 92 (1988) 5851.
[r100] N. Shinyashiki, M. Shimomura, T. Ushiyama, T. Miyagawa, S. Yagihara, J. Phys. Chem. B, 111 (2007) 10079.
[r101] R. Buchner, J. Barthel, J. Stauber, Chem. Phys. Lett. 306 (1999) 57.
[r102] A. Buchsteiner, A. Lerf, J. Pieper, J. Phys. Chem. B., 110 (2006) 22328.
[r103] A. Lerf, A. Buchsteiner, J. Pieper, S. Schottl, I. Dekany, T. Szabo, H.P. Boehm, J. Phys.Chem. Solids, 67, 106 (2006).
[r104] T. Becker, J. A. Hayward, J. L. Finney, R. M. Daniel, J. C. Smith, Biophysical J. 87 (2004) 1436.
[r105] M. Jasnin, L. van Eijck, M. Marek Koza, J. Peters, C. Laguri, H. Lortat-Jacob, G. Zaccai, Phys. Chem. Chem. Phys. 12 (2010) 3360.
[r106] S. Sacquin-Mora, P. Sebban, V. Derrien, B. Frick, R. Lavery, Ch. Alba-Simionesco, Biochemistry 46 (2007) 14960.
[r107] I. Köper, S. Combet, W. Petry, M.-C. Bellissent-Funel, Eur Biophys J. 37 (2008) 739.
[r108] S. Magazú, F. Migliardo, C. Mondelli, M. Vadala, Carbohydrate Res. 340 (2005) 2796.
[r109] E. Cornicchi, S. Capponi, M. Marconi, G. Onori, A. Paciaroni, Philos.Mag. 87 (2007) 509.
[r110] G. Schiro, M. Sclafani, C. Caronna, F. Natali, M. Plazanet, A. Cupane, Chem. Phys. 345 (2008) 259.
[r111] A. M. Tsai, T. J. Udovic, D. A. Neumann, Biophysical J. 81 (2001) 2339.
[r112] T. Kleinert, W. Doster, H. Leyser, W. Petry, V. Schwarz, M. Settles, Biochemistry 37 (1998) 717.
[r113] H. Lichtengegger, W. Doster, T. Kleinert, A. Birk , B. Sepiol, G. Vogl, Biophys.J. 76 (1999) 414
[r114] R. Casalini, K. L. Ngai, C. M. Roland, Phys.Rev.B 68 (2003) 014201
[r115] L. Cordone, M. Ferrand, E. Vitrano, G. Zaccai, Biophys. J. 76 (1999) 1043.
[r116] K. Kaminski, E. Kaminska, P. Wlodarczyk, S. Pawlus, D. Kimla, A. Kasprzycka, M. Paluch, J. Ziolo, W. Szeja, K. L. Ngai, J. Phys. Chem. B 112 (2008) 12816.
[r117] J. L Green, C. A. Angell, J. Phys. Chem. 93 (1989) 2880.
[r118] C. Branca, S. Magazu, G. Maisano, P. Migliardo, J. Chem. Phys. 111 (1999) 281.
[r119] R. M. Daniel, J. L. Finney, and J. C. Smith, Faraday Discuss. 122 (2003) 163
[r120] K.L. Ngai and C.M. Roland, Rubber Chem. Technol. 77 (2004) 579 and references therein
[r121] R. S. Smith, B. D. Kay, Nature 398 (1999) 788
[r122] C.A. Angell, Chem. Rev. 102 (2002) 2627-2650